NASA
Reference
Publication
1241

July 1990

Sensor Performance Analysis

H. E. Montgomery,
H. Ostrow,
and G. M. Ressler

NASA

NASA
Reference
Publication
1241

1990

Sensor Performance Analysis

H. E. Montgomery
and H. Ostrow
Goddard Space Flight Center
Greenbelt, Maryland

G. M. Ressler
Ressler Associates, Inc.
Laurel, Maryland

NASA

National Aeronautics and
Space Administration
Office of Management
Scientific and Technical
Information Division

CONTENTS

LIST OF SYMBOLS

A = Overlap factor across track, given by Equation (C-9) in Appendix C.

A_o = Sensor entrance aperture area (cm^2).

A_D = Detector area (m^2).

A_I = The area of the ground resolution element (km^2), used in Equation (A-2).

A_m = A function used in the MTF_{OA} computation, Equation (7-2).

B = Overlap factor along track, given by Equation (4-9).

$B(\lambda)$ = Planck's spectral distribution of radiation (W/cm^2–sr–μm) from a blackbody, given by Equation (3-5).

$B'(\lambda)$ = Planck's spectral distribution of radiation (p/sec–cm^2–sr–μm) from a blackbody, given by Equation (3-7).

B_m = A function used in the MTF_{OA} computation, Equation (7-2).

c = Speed of light = 2.998×10^{10} (cm/sec).

C = A constant used in Equation (2-8).

C_1 = $2\pi hc^2$ = A constant used in the computation of $B(\lambda)$.

C_o = Output capacitance.

C_m = A function used in the MTF_{OA} computation, Equation (7-2).

C'_1 = $2\pi c$ = A constant used in the computation $B'(\lambda)$.

C_2 = hc/k_B = A constant used in the computation of $B(\lambda)$ and $B'(\lambda)$.

d_C = Distance covered cross track during the time required to map the Earth t_M, given by Equation (C-6).

D = Aperture diameter of the sensor, used in Equation (A-7).

D^* = Specific detectivity (laboratory or handbook value), defined in Equation (5-20).

D^*_{BLIP} = Background-limited value of D^*, given by Equation (5-33).

d = Photodetector depletion region depth, used in Equation (7-19).

d_m = Distance moved by the satellite along the ground track during one scan period, given by Equation (4-7).

d_C = The extent imaged along the ground track at nadir during one scan mirror period,

PRECEDING PAGE BLANK NOT FILMED

PAGE iv INTENTIONALLY BLANK

given by Equation (4-6).

d_S	=	Width of square detector (μm).
$d\lambda$	=	Differential of wavelength λ.
$E(\lambda)$	=	Scene spectral irradiance (W/cm^2-μm) into the detector, given by Equation (2-10).
$E'(\lambda)$	=	Scene spectral irradiance (p/sec-m^2-μm) into the detector, given by Equation (2-6).
E'_{BG}	=	The irradiance at the infrared detector from the scene and the background, given by Equation (5-25).
E_G	=	Silicon band gap (e-v) used in Equation (5-6a).
F_M	=	A factor used in Equation (4-5) to distinguish between a 45-degree scan mirror and a paddle scan mirror.
$E_{\lambda o}$	=	Spectral irradiance (mw/cm^2-μm) of the direct sunlight above the atmosphere, used in Equation (B-2).
$E_{\lambda s}$	=	The solar irradiance (mw/cm^2) of the direct sunlight at sea level, used in Equation (B-2).
f	=	Focal length (cm), used in Equation (A-6).
F_A	=	View factor for a detector in an n by m array viewing a rectangular background, given by Equation (E-1), in Appendix E.
F_L	=	View factor of the detector in the laboratory where D* was measured, given by Equation (5-19).
F_C	=	View factor for a cold shielded detector viewing the scene through a circular aperture, given by Equation (5-29).
f_N	=	The f-number (nd) of the optical system, given by Equation (A-9).
g_m	=	Transconductance.
J_0	=	Zeroth-order Bessel function, used in Equation (7-26).
J_{DC}	=	Dark current density (a/cm^2), given by Equation (5-6a).
H	=	Satellite height (km).
h	=	Planck's constant = 6.626×10^{-34} (W-sec^2).
k	=	Spatial frequency (cycles/mm).
k_0	=	$1/2\lambda f_N$, used in the MTF_{OA} computations and given by Equation (7-12).

k_B = Boltzmann's constant = 1.380×10^{-23} (W-sec/K).

k_C = $2k_o$ = Cutoff frequency, used to compute MTF_{OA} in Equation (7-13).

L = A function used in the MTF_{CT} and given by Equation (7-22).

L_0 = Diffusion length, used in Equation (7-22).

$L(\lambda)$ = Scene spectral radiance (W/cm^2–sr–μm), given by Appendix B for the visible bands and by Equation (3-2) for the infrared bands.

$L'(\lambda)$ = Scene spectral radiance (p/sec–cm^2–sr–μm), given by Equation (2-12).

L_A^N = Spectral radiance (W/cm^2–sr–μm) from the atmosphere observed by the sensor when viewing along the nadir direction, used in Equation (B-4).

L^N = Total spectral radiance (W/cm^2–sr–μm) observed by the sensor when viewing along the nadir direction, given by Equation (B-4).

L_S = Spectral radiance (W/cm^2–sr–μm) observed by the sensor which comes from the surface of the Earth, used in Equation (B-4).

M = Mass of the Earth (kg).

M_{CT} = Total number of charge transfers, used in Equation (7-23).

M_g = Number of gate transfers.

MTF = Modulation transfer function, given by Equation (7-1).

MTF_{CT} = Charge transfer MTF, given by Equation (7-23).

MTF_{DA} = Detector aperture MTF, given by Equation (7-16).

MTF_{OA} = Optical aperture MTF, given by Equation (7-2).

MTF_{SJ} = Satellite jitter MTF, given by Equation (7-26).

MTF_{SM} = Satellite motion MTF, given by Equation (7-17).

m = Mass of the electron = 9.1×10^{-31} (kg).

m_P = Number of clock phases for readout, used in Equation (7-24).

m_S = Number of stages, detectors or picture elements, used in Equation (7-24).

N_{BT} = Bulk trap noise (e), given by Equation (5-3).

N_{CT} = Charge transfer noise (e), given by Equation (5-11).

N_{DC} = Dark current noise (e), given by Equation (5-5).

N_{DCS} = Dark current noise (e) for a Schottky barrier detector, given by Equation (5-9).

N_{DET} = Detector noise (e), used in Equations (5-1) and (5-16).

NEE = Noise equivalent electrons (e), given by Equation (5-21).

NEP = Noise equivalent power (W), given by Equation (5-20).

$NE\Delta T$ = Noise equivalent delta temperature (K), given by Equation (6-5).

$NE\Delta\rho$ = Noise equivalent delta reflectance (nd), given by Equation (6-1).

N_M = Multiplexer noise (e).

N_{OA} = Output amplifier noise (e), given by Equation (5-4).

N_{OD} = Other detector noise (e), given by Equation (5-17).

N_{OS} = Other system noise (e).

N_P = Photon noise (e), given by Equation (5-2) for the visible domain and by Equation (5-23) for the infrared domain.

N_{PL} = Photon noise (e) under laboratory conditions, given by Equation (5-18).

N_Q = Quantization noise (e), given by Equation (5-12) for the visible domain and by Equation (5-34) for the infrared domain.

N_T = Thermal (Johnson) noise (e), given by Equation (5-8).

N_{TOT} = Total noise from all sources (e), given by Equation (5-1).

N_{SYS} = System noise (e), used in Equation (5-1).

n = Size distribution function for aerosol particles, used in Equation (B-3).

n_D = Number of detectors per spectral band.

n'_D = Number of detectors along an array, used to compute the charge transfer noise in Equation (5-11).

n_E = Number of resolution elements along a scan line, given by Equation (4-1).

n_f = Number of facets in a 45-degree scan mirror.

n_P = The number of phases used to transfer charge along a detector array, used in Equation (5-11).

n_S = A factor used in Equation (4-14) to distinguish between imaging in one scan mirror direction and imaging in both scan mirror directions.

n_{SS} = Density of surface states, used in Equation (5-3).

P_D = Detector pitch (μm).

Q = Number of bits used in the analog-to-digital converter.

q = Charge of an electron = 1.602×10^{-19} (Coul).

R = Resistance (ohms).

$R(\lambda)$ = Detector current responsivity (A/W), given by Equation (2-3).

R_C = $4\pi qmk^2/h^3$ = Richardson constant (a/cm^2-K^2), used in Equation (5-9a).

R_e = 6378.165 (km) = Radius of the Earth.

R_S = Distance (km) from the center of the Earth to the satellite, given by Equation (B-2).

r = Radius of aerosol particle, used in Equation (B-3).

S = Signal (A) from the detector, given by Equation (2-2).

S_F = Saturation factor, defined by Equation (5-14).

S′ = Signal (e) from the detector, given by Equation (2-7).

S'_{SAT} = The saturation signal (e), given by Equation (5-13).

S_d = Distance (km) from the satellite to the point on the Earth that corresponds to the maximum scan angle, given by Equation (C-3).

S_W = Swath width (km) on the Earth, given by Equation (C-5).

S_o = Percentage overlap along track, used in Equation (4-10).

S'_o = Percentage overlap across track, used in Equation (C-9).

T = Blackbody temperature (K).

T_{BG} = Background temperature for the sensor (K).

T_{BGL} = Background temperature (K) when D* is measured in the laboratory.

T_S = Earth's surface temperature (K).

T_A = Earth's atmospheric temperature (K).

t_A = Active scan time, which is that part of the scan mirror period when data are being acquired, given by Equation (4-4).

t_I = Detector integration time (sec), given by Equation (2-8).

t_D = Detector dwell time (sec), given by Equations (4-3) and (4-12) for a spinning scan mirror; Equations (4-14) and (4-17) for a rocking scan mirror; and by Equation (4-18) for a linear array.

t_M = Period of the scan mirror (sec), given by Equation (4-11) for a spinning mirror and by Equation (4-16) for a rocking scan mirror.

t_{MAP} = Time to map the Earth (days).

t_S = Satellite orbital period (sec), given by Equation (C-8).

V_{SUB} = The velocity (km/sec) of the subsatellite point, given by Equation (4-8).

V_I = Image velocity (km/sec), given by Equation (7-18).

z = A curve-fitted function used to compute the silicon absorption coefficient, given by Equation (7-21).

α = Instantaneous angular field of view (r), given by Equation (4-2).

α_a = Silicon absorption coefficient (nd), used in Equation (7-19).

α_M = A material-dependent factor used in Equation (5-6a).

β = D_o/D, used in the MTF_{OA} computations, given by Equation (7-15).

γ = $(S/N) \cdot NE\Delta\rho$ and is given by Equation (6-2).

γ_o = $(S/N) \cdot NE\Delta\rho$ along nadir and is given by Equation (6-3).

Δf = Electrical bandwidth (Hz), given by Equation (5-22).

$\Delta\lambda$ = $\lambda_2 - \lambda_1$ = Spectral bandpass (μm).

δ_A = Optical thickness (nd) of the aerosols, used in Equation (B-1).

δ_G = Optical thickness (nd) of the absorbing gases, used in Equation (B-1).

δ_R = Optical thickness (nd) due to Rayleigh scattering, used in Equation (B-1).

δ_T = Optical thickness (nd).

δ_{TN} = Optical thickness (nd) in the nadir direction, used in Equations (6-4) and (B-1).

η = Detector quantum efficiency (nd).

η_M = A material-dependent carrier recombination factor, used in Equation (5-6a).

ϵ = Charge transfer inefficiency (nd), used to compute MTF_{CT}.

ϵ_A = Emissivity of the atmosphere (nd).

Θ = Field-of-view (FOV) angle (deg) subtended by the swath width at the satellite. It is given by Equation (4-8) for a linear array and by Appendix C [Equation (C-1)] for whiskbroom (scanning) systems.

Θ_M = Maximum satellite angular movement (rad) used to compute jitter MTF in Equation (7-26).

θ = Optics half-cone angle (deg), given by Equation (A-10).

θ_{BG} = The full-cone angle (deg) of the background used in Equation (5-29).

θ_z = Solar zenith angle (deg), angle between Earth normal and Sun direction, used in Table B-2.

κ = Scan efficiency (nd), given by Equation (4-5) for spinning mirrors.

π = The well-known ratio between the circumference and the diameter of a circle, 3.14159 (nd).

λ = Center wavelength of a spectral band (μm).

Λ = k/k_o, used in the MTF_{OA} computations.

λ_1 = Lower wavelength of a spectral band (μm).

λ_2 = Upper wavelength of a spectral band (μm).

μ = GM, the product of the gravitational constant G and the mass of the Earth M $= 3.98603 \times 10^5$ (km^3-sec^{-2}).

ρ = Reflectance of the Earth's surface (nd).

τ = Transmittance (nd) of the atmosphere in the visible spectral region, given by Equation (B-2).

τ' = Total number of electrons produced by an infrared detector from the scene and the background, given by Equation (5-24).

τ_A = Transmittance (nd) of the atmosphere, used for the infrared spectral region.

τ_{AN} = Optical transmittance (nd) along the nadir direction, given by Equation (6-4).

τ_o = Optical transmittance (nd) from the sensor entrance aperture to the detector, used in Equation (5-26).

Φ	=	Power (W) incident on the detector, given by Equation (2-1).
Φ'	=	Photon flux incident on the detector (p/sec).
Φ_S	=	Angle (deg) subtended at the satellite by ground swath, given by Equation (C-4).
ϕ_C	=	Cone angle (deg) for detector view, used in Equation (5-19).
ϕ_f	=	The angle between the normal to the differential area dA_B and the line between the center of the detector and the center of the area dA_B, used in Appendix F.
ϕ_m	=	A function that when multiplied by the charge of an electron q, gives the work function of the metal in the semiconductor. It is used in Equation (5-9a).
ϕ'	=	The angle (deg) between the line of sight and the surface normal, used in Equation (6-2).
ψ	=	A function used in the MTF_{OA} computation, given by Equation (7-10).
Ω	=	The effective solid angle (sr) through which the detector receives energy from the resolution element, given by Equation (5-27).
Ω_o	=	Effective solid angle (sr) subtended by the entrance aperture at the subsatellite point, used in Equation (A-7).
Ω_{BG}	=	Effective solid angle (sr) of the background, given by Equation (5-28).

1. INTRODUCTION

The purpose of this paper is to present an analytic model of an imaging sensor system so that: (1) sensor performance predictions can be made; (2) design tradeoffs and sensitivity analyses can be rapidly performed; and (3) insight into various aspects of imaging sensor performance can be obtained. The model is applicable to image sensors which operate from the visible through the thermal infrared spectral regions.

The design of sensors for remote observation of the Earth from polar orbiting satellites takes about a decade and occurs in five different stages. These stages are:

- *Definition of Scientific Requirements.* During this stage, scientific working groups formulate the scientific requirements (e.g., spatial, temporal, and spectral resolution; measurement accuracy, etc.)
- *Preliminary Design.* During this stage a "paper design" is developed. (Determination is made of such parameters as f-number, detector size, and number of detectors) that permit the sensor to meet the scientific requirements (e.g., signal-to-noise ratio, noise-equivalent delta temperature, or noise-equivalent delta reflectance).
- *Feasibility Studies (Phase B).* During this stage, engineering feasibility is established without regard to optimization of the design.
- *Design Studies (Phase B).* During this phase, the design is optimized, and an in-depth analysis is performed on each subsystem (e.g., optics, focal plane, cooler, electronics, mechanical systems) and a credible cost estimate is produced.
- *Flight Hardware Design, Development, Test and Integration into the Space Platform (Phase C/D).* During this stage, flight hardware is designed, developed, and tested to prove that it meets the specification, and is integrated into the space platform.

Only Preliminary Design (the second stage) is addressed in this document. Derivations or references are given for all the equations to make it easy to change the theory as required in future applications.

The spectral range is limited to 0.4 to 15.0 μm which is generally appropriate for studies of the Earth and its environment. The types of scanners include the "pushbroom" and two different kinds of "whiskbrooms." A substantial portion of the analysis presented herein has been incorporated into a self-documented Lotus 1-2-3 spreadsheet.

Analytic (as opposed to statistical) methods are used in the model. Analyses are carried out at very low spatial (and therefore temporal) frequencies in order to simplify the computations. High spatial frequencies are used only to determine the MTF of the sensor. Carrying out the analyses at low spatial frequencies also avoids the necessity of working in the frequency domain which generally involves fourier transformations or convolutions in the time domain, and would therefore make the sensor model very complex. To further simplify the analyses, it is also assumed that the sensors have narrow spectral bandwidths so that those parameters that are spectrally dependent (e.g., detector responsivity) can be reduced to a constant.

The model assumes that the sensor is a linear system from the optical input through the electronic signal processing. This assumption is satisfied if (1) the optical system is not dominated by diffraction effects; (2) incoherent detection methods are employed; (3) the various noise sources are additive in an rss sense; (4) the imaging process is spatially invariant; and (5) the electronic signal processing constitute linear operations. These assumptions are all valid for the types of imaging sensors that the model is presently being applied to.

Appropriate scene radiance levels must be assigned in order to assess sensor system performance. In the model described in this document, tables are included which allow a user to determine radiances at the top of the Earth-atmosphere system as a function of wavelength. These tables apply to the visible and near ir spectral regions. The origin of the tables is discussed in Appendix B. For the thermal infrared region, radiances are directly computed.

Section 2 addresses the power incident on the detector during an observation interval and the signal coming out the detector. These are written as functions of the irradiance at the detector and as a function of the scene radiance.

Section 3 provides a description of the model used for the scene radiance.

Section 4 derives the equations for detector dwell time for four different scanning configurations which include: a spinning 45-degree scan mirror, a spinning paddle mirror, a rocking scan mirror, and a linear array-pushbroom.

Section 5 is devoted to the major noise sources associated with visible and infrared detectors.

Section 6 presents definitions and derivations of various "figures of merit" including Noise Equivalent Delta Reflectance (NE$\Delta\rho$) and Noise Equivalent Delta Temperature (NEΔT).

Section 7 develops the Modulation Transfer Function (MTF) for the optical aperture, the detector aperture, satellite motion, charge diffusion, charge transfer, and satellite jitter.

The Appendixes treat many of the equations in a tutorial manner.

2. POWER AND SIGNAL

When viewing the scene, the power (flux) into the detector is given by

$$\Phi = A_D \int_{\lambda_1}^{\lambda_2} E(\lambda)\, d\lambda \qquad [W], \tag{2-1}$$

where A_D = the area of the detector (cm^2);

$E(\lambda)$ = scene spectral irradiance at the detector (W/cm^2-μm);

λ = center wavelength of spectral band (μm); and

$\Delta\lambda$ = $\lambda_2 - \lambda_1$ = spectral bandpass (μm).

The signal out of the detector is given by

$$S = A_D \int_{\lambda_1}^{\lambda_2} E(\lambda) R(\lambda)\, d\lambda \qquad [A], \tag{2-2}$$

where $R(\lambda)$ is the detector current responsivity and is given by

$$R(\lambda) = \frac{q\eta}{hc} \lambda \qquad [A/W], \tag{2-3}$$

where q = the charge of an electron = 1.60×10^{-19} [coul];

η = the detector quantum efficiency [nd] (assumed to be constant over the spectral bandpass $\Delta\lambda$);

h = Planck's constant = 6.63×10^{-34} [Wsec^2]; and

c = the speed of light = 3.00×10^{10} [cm/sec].

Substituting Equation (2-3) into Equation (2-2) gives

$$S = \frac{A_D q \eta}{hc} \int_{\lambda_1}^{\lambda_2} E(\lambda) \lambda\, d\lambda \qquad [A]. \tag{2-4}$$

Equation (2-4) may be written in terms of the spectral photon irradiance as

$$S = A_D \, q\eta \int_{\lambda_1}^{\lambda_2} E'(\lambda) \, d\lambda \qquad [A], \tag{2-5}$$

where the scene spectral photon irradiance $E'(\lambda)$ at the detector is given by

$$E'(\lambda) = \frac{\lambda}{hc} \; E(\lambda) \qquad [p/sec\text{-}cm^2\text{-}\mu m] \; . \tag{2-6}$$

The signal out of the detector is given by

$$S' = \frac{t_I}{q} \; S \qquad [e], \tag{2-7}$$

where the integration time t_I is given by

$$t_I = Ct_D \qquad [sec], \tag{2-8}$$

where C is an input constant and t_D is the sensor dwell time, which is described in detail in Section 4.

Substituting Equation (2-5) into Equation (2-7) gives

$$S' = t_I \; A_D \; \eta \int_{\lambda_1}^{\lambda_2} E'(\lambda) \, d\lambda \qquad [e] \; . \tag{2-9}$$

The scene spectral irradiance at the detector is related to the scene spectral radiance by the following two equations given in terms of watts and photons, respectively. (See Appendix A.) The first equation is

$$E(\lambda) = \frac{\tau_o \pi}{4f^2_N} \; L(\lambda) \qquad [W/cm^2\text{-}\mu m], \tag{2-10}$$

where τ_o = the optical transmittance [nd] from the sensor aperture to the detector, and

f_N = f-number of the optics [nd] .

The second equation is

$$E'(\lambda) = \frac{\tau_o \pi}{4f^2_N} \; L'(\lambda) \qquad [p/sec\text{-}cm^2\text{-}\mu m] \; . \tag{2-11}$$

Also, for completeness, note that

$$L'(\lambda) = \frac{\lambda}{hc} \; L(\lambda) \qquad [\mathrm{p/cm^2\text{-}sec\text{-}sr\text{-}\mu m}] \; . \tag{2-12}$$

For the visible and shortwave infrared (SWIR) wavelengths, it is assumed that the spectral bandpass $\Delta\lambda$ is small and that the scene spectral photon irradiance $E'(\lambda)$ varies slowly over $\Delta\lambda$. In this case, the integration in Equations (2-1) and (2-4) can then be approximated by $E'\Delta\lambda$, where E' is the average value of $E(\lambda)$ over the spectral bandpass $\Delta\lambda$.

3. SPECTRAL RADIANCE

In this section, we will show how to obtain the spectral radiance for the visible and SWIR spectral wavelengths (0.4 to 2.2 μm) and the infrared spectral wavelengths (2.2 to 15 μm).

3.1 Visible and Shortwave Infrared (SWIR) Spectral Radiance

A table of values of the scene spectral radiance at the sensor aperture is given in Appendix B as a function of ρ, θ_z, and λ

where ρ = Earth's surface reflectance (nd), and

θ_z = solar zenith angle (deg).

The scene spectral radiance $L(\lambda)$ is obtained from the tables by trilinear interpolation at the desired values of ρ, θ_z, and λ. Although the values of scene spectral radiance in the tables were computed for a nadir viewing sensor, we assume that the values are independent of viewing angle. (See Equation C-4).

3.2 Infrared Spectral Radiance

The total scene spectral radiance in the infrared is given by

$$L(\lambda) = \tau_A \ B(\lambda,T_S) + \epsilon_A \ B(\lambda,T_A) \quad [\text{W/cm}^2\text{-sr-}\mu\text{m}] \tag{3-2}$$

where τ_A is the atmospheric transmittance for an optical depth δ, given by

$$\tau_A = e^{-\delta} \tag{3-3}$$

and where ϵ_A is the atmospheric emissivity given by

$$\epsilon_A = 1 - \tau_A \tag{3-4}$$

The quantities $B(\lambda,T_S)$ and $B(\lambda,T_A)$ are the spectral radiances of the Earth's surface at temperature T_S and the atmosphere at temperature T_A, respectively, and are given by Planck's equation (Hudson, 1969, p. 35) for a blackbody at temperature T,

$$B(\lambda,T) = \frac{C_1}{\pi\lambda^5} \frac{1}{\exp\left(\frac{C_2}{\lambda T}\right) - 1} \quad [\text{w/cm}^2\text{-sr-}\mu\text{m}] \tag{3-5}$$

where Hudson's equation (2-8) has been divided by π to convert to radiance, and where

C_1 = $2\pi hc^2 = 3.74 \times 10^4$ [W-μm^4/cm^2];

h = Planck's constant = 6.63×10^{-34} [W-sec^2];

c = speed of light = 2.998×10^{10} [cm/sec];

C_2 = $hc/k_B = 1.44 \times 10^4$ [μm-K];

k_B = Boltzmann's constant = 1.38×10^{-23} [W-sec/K]; and

T = Blackbody temperature [K].

The total scene spectral photon radiance is given by

$$L'(\lambda) = \tau_A \, B'(\lambda,T_S) + \epsilon_A \, B'(\lambda,T_A) \qquad [\text{p/sec-cm}^2\text{-sr-}\mu\text{m}], \tag{3-6}$$

where the surface spectral photon radiance $B'(\lambda,T_S)$ and the atmospheric spectral photon radiance $B'(\lambda,T_A)$ are found by evaluating the following equation (Hudson, 1969, p. 38) at T_S and T_A, respectively:

$$B'(\lambda,T) = \frac{C'_1}{\pi\lambda^4} \frac{1}{\left(\exp\left(\frac{C_2}{\lambda T}\right) - 1\right)} \quad [\text{p/sec-cm}^2\text{-sr-}\mu\text{m}] \tag{3-7}$$

where

$$C'_1 = 2\pi c = 1.88 \times 10^{23} \ [\text{p-sec}^{-1}\text{-cm}^{-2}\text{-}\mu\text{m}^3]$$

4. DWELL TIME

As the satellite moves in orbit, it images along scan lines perpendicular to the ground track. Let the extreme ends of the scan lines on the Earth subtend an angle Θ at the satellite. This angle is called the field-of-view (FOV). See Figure 1 for an illustration of the geometry involved and refer to Appendix C for a discussion of the relations between the parameters shown in the figure. The number of angular resolution elements n_E is given by

$$n_E = \frac{\Theta}{\alpha} \text{ [nd]} \tag{4-1}$$

and (as can be seen from Figure 1) the instantaneous angular field of view α (geometric only) is given by

$$\alpha = \frac{d_S}{f} \text{ [rad]} \tag{4-2}$$

where d_S = detector width (mm), and

f = focal length of the optical system (mm).

A scan line can be formed by a spinning mirror, a rocking mirror, or a linear array. Each of these are discussed in the following sections.

4.1 Spinning Mirror

Two types of spinning mirrors are discussed in this section: the 45-degree scan (faceted) mirror and the paddle scan mirror (Figures 2a and 2b). The axis of rotation for a 45-degree scan mirror is parallel to the sensor's optical axis, and a change in the angle of rotation of θ will produce an equal change in the line-of-sight angle. The axis of rotation for a paddle scan mirror is perpendicular to the sensor's optical axis, and therefore, a change in the angle of rotation of θ will result in a 2θ change in the line-of-sight angle.

The dwell time for a spinning mirror is given by

$$t_D = \frac{t_A}{n_E n_f} \text{ [sec]}, \tag{4-3}$$

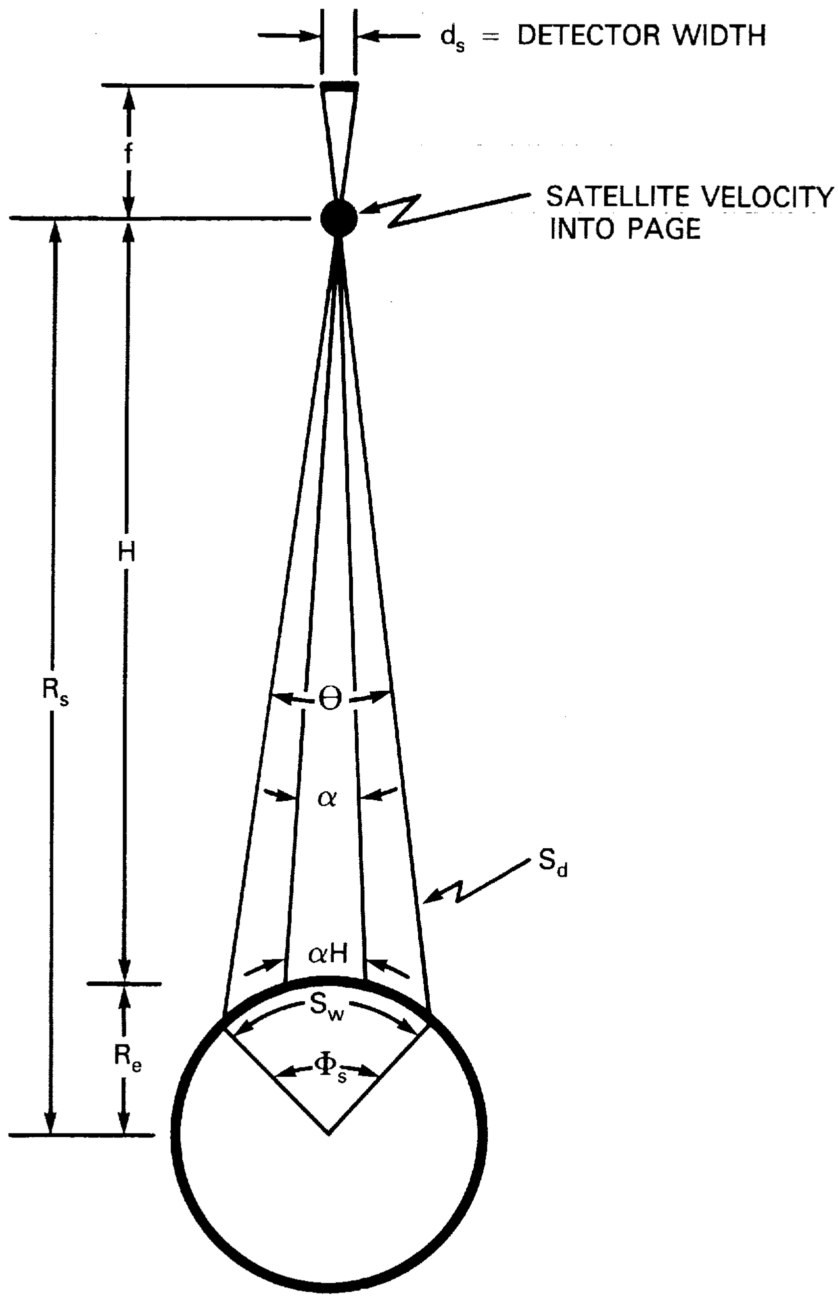

d_s = Width of square detector (μm)
f = Focal length (cm)
H = Satellite height (km)
R_e = Radius of Earth (km)
R_s = Earth-to-satellite distance (km)
S_d = Maximum scan angle distance (km)
α = Instantaneous angular FOV (deg)
Θ = Swath width FOV (deg)
Φ_s = Ground swath angle (deg)
S_w = Swath width (km)

Figure 1. FOV and IFOV Geometry

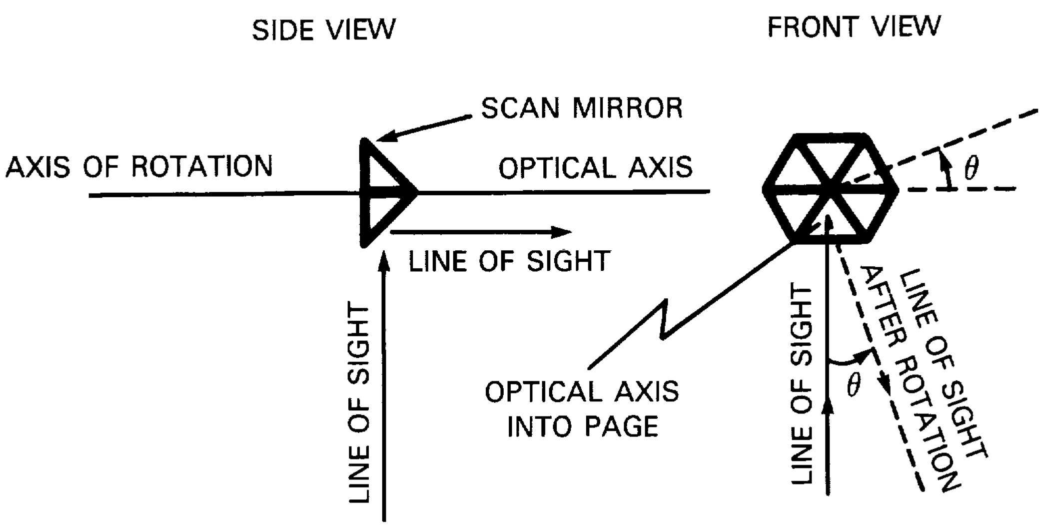

*NOTE: AS MIRROR ROTATES THROUGH AN ANGLE θ THE LINE OF SIGHT ALSO ROTATES THROUGH AN ANGLE θ

Figure 2a. Scan Mirror Geometry for 45-Degree Faceted Scan Mirror

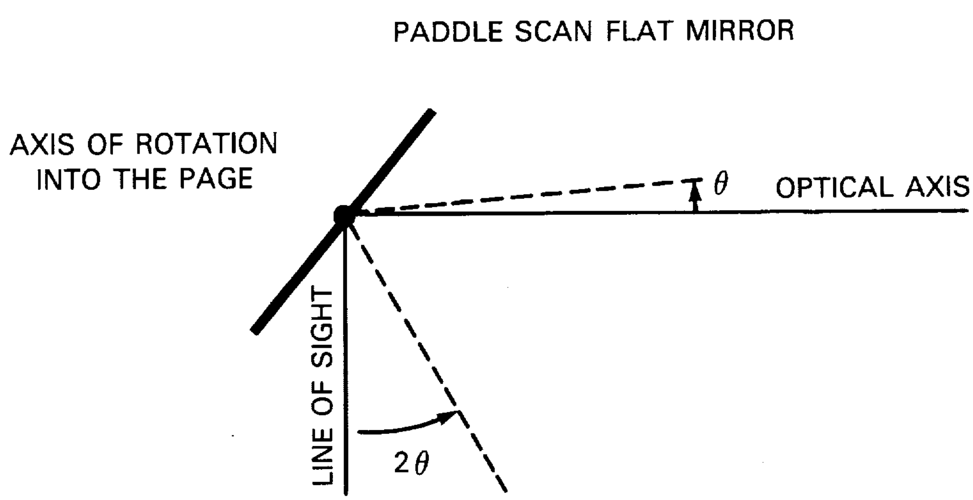

*NOTE: AS THE MIRROR ROTATES THROUGH AN ANGLE θ THE LINE OF SIGHT ROTATES THROUGH AN ANGLE 2θ

Figure 2b. Scan Mirror Geometry for Paddle Scan Flat Mirror where n_f = the number of facets,

$$n_f \begin{cases} \geqslant 1 & \text{for a 45-degree scan mirror, and} \\ = 1 & \text{for a paddle scan mirror.} \end{cases}$$

The active scan time t_A, which is that part of the scan mirror period during which data are acquired, is given by

$$t_A = \kappa t_M \quad [\text{sec}], \tag{4-4}$$

where the scan mirror period t_M is the time for the spinning scan mirror to make a complete revolution, and the scan efficiency κ is given by

$$\kappa = \frac{n_f \Theta}{2\pi F_M} \quad [\text{nd}], \tag{4-5}$$

where $F_M \begin{cases} = 1 & \text{for a 45-degree scan mirror,} \\ = 2 & \text{for a paddle scan mirror.} \end{cases}$

During each scan, an area on the ground is imaged. The extent imaged along the ground track at nadir (Figures 3 and 4) is

$$d_C = n_f n_D \alpha H \quad [\text{km}], \tag{4-6}$$

where H = the satellite height [km], and

n_D = the number of detectors per spectral band.

Also, during each scan, the satellite moves a distance d_m measured along the ground track, which is given by

$$d_m = t_M V_{SUB} \quad [\text{km}], \tag{4-7}$$

where V_{SUB} is the speed of the subsatellite point along the ground track and is given by

$$V_{SUB} = R_e \frac{(\mu)^{1/2}}{(R_e + H)^{3/2}} \quad , \tag{4-8}$$

where

$$\mu = GM = 3.98603 \times 10^5 \ (\text{km}^3\text{-sec}^{-2})$$

where G is the universal gravitational constant, and M is the mass of the Earth.

The overlap factor B is given by

$$B = \frac{d_C}{d_m} \quad [\text{nd}], \tag{4-9}$$

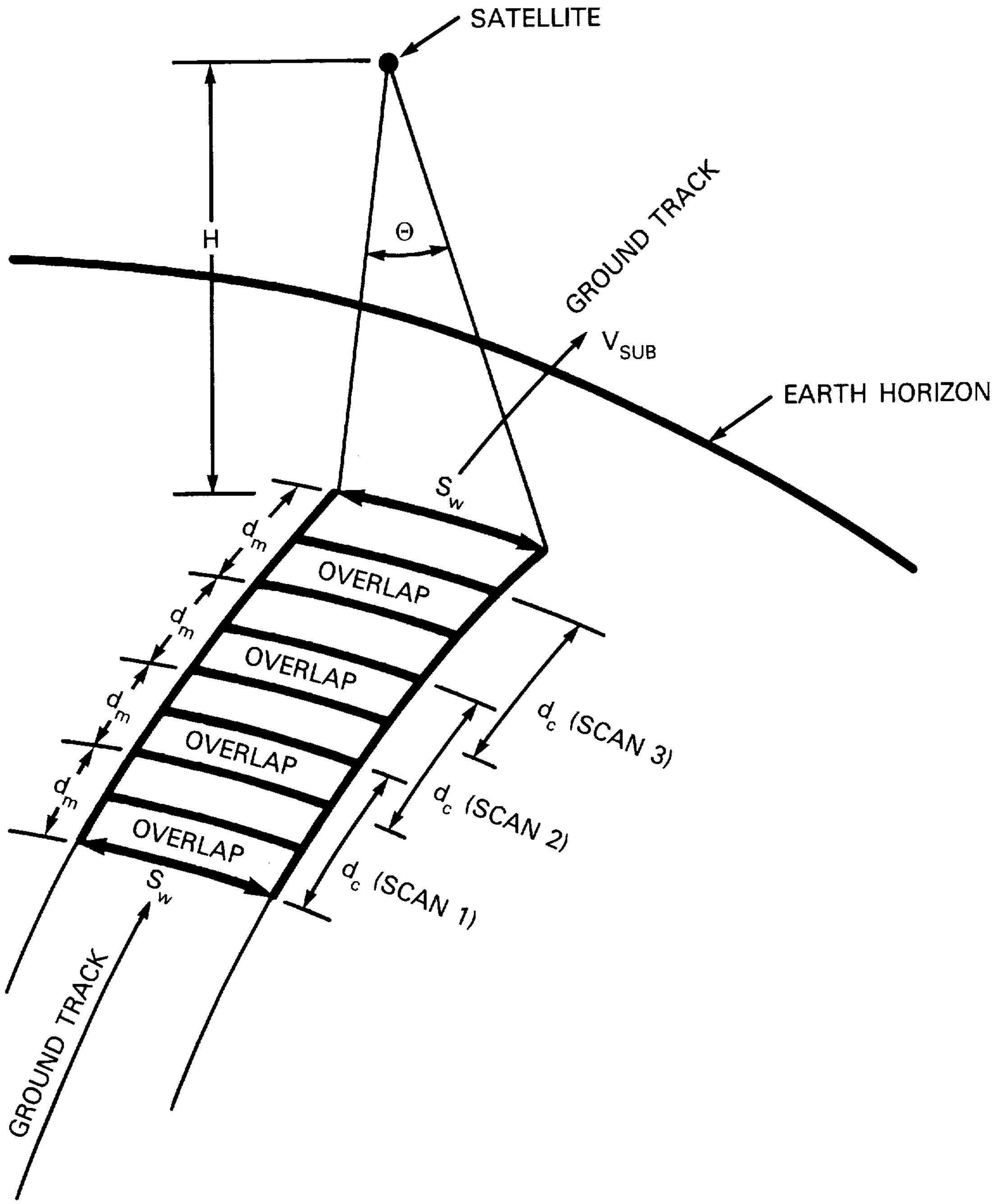

d_m = Ground distance moved per scan period (m)
d_c = Extent imaged along ground track per scan period (m)
Θ = Swath width FOV (deg)
H = Satellite height (km)
S_w = Swath width
V_{SUB} = Subsatellite velocity (km/sec)

Figure 3. Ground Track and Scanning Geometry

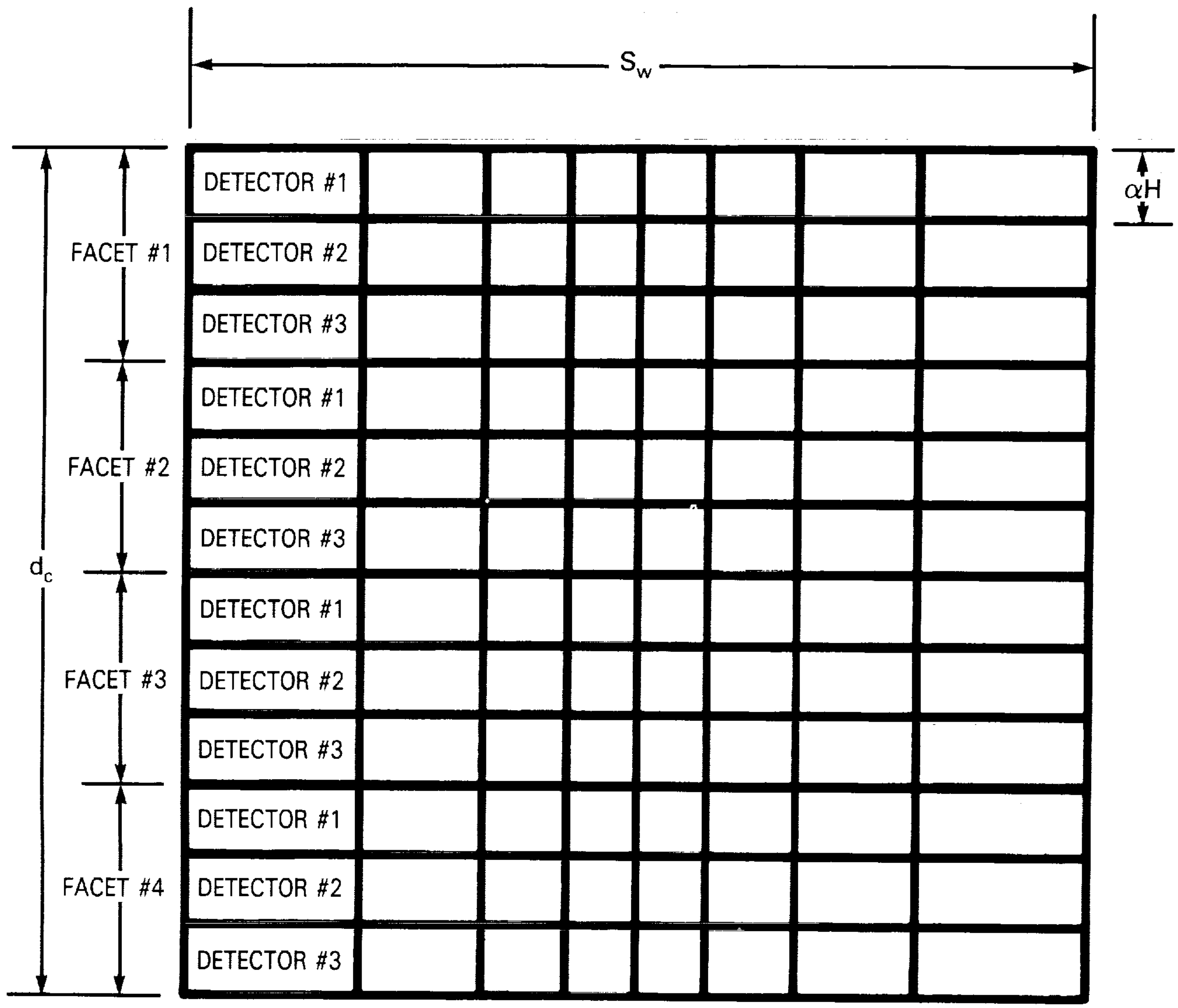

n_f = 4 = Number of facets on scan mirror
n_D = 3 = Number of detectors per spectral band
H = Satellite height (km)
S_w = Swath width (km)
α = Instantaneous angular FOV (as in Fig. 1) (deg)
d_c = Extent imaged along ground track per scan (m)

Figure 4. Example of Scanning Geometry for a 45-Degree Faceted Scan Mirror

where B = 1 for contiguous coverage, B > 1 for overlap, and B < 1 for incomplete coverage (underlap). In terms of the percentage of overlap S_o we may write

$$B = 1 + \frac{S_o}{100} \quad [\text{nd}] \ . \tag{4-10}$$

Using Equations (4-7), (4-9), and (4-6), one obtains

$$t_M = \frac{n_f n_D \alpha H}{B V_{SUB}} \quad [\text{sec}] \ . \tag{4-11}$$

However, from Equations (4-1), (4-3), (4-4), and (4-5), t_D may be written as

$$t_D = \frac{\alpha}{2\pi F_M} t_M \quad [\text{sec}] \ . \tag{4-12}$$

From Equation (4-12) it can be seen that t_D is independent of the field of view Θ, and therefore, changing the swath width does not change the dwell time. Substituting Equation (4-11) into (4-12) yields

$$t_D = \frac{\alpha}{2\pi} \frac{n_f n_D \alpha H}{B V_{SUB} F_M} \quad [\text{sec}] \ . \tag{4-13}$$

4.2 Rocking Mirror

During a complete cycle, the rocking mirror rotates back and forth through an angle that covers the FOV Θ twice–once in each direction. For this case, the dwell time is

$$t_D = \frac{t_A}{n_S \, n_E} \quad [\text{sec}] \tag{4-14}$$

where n_S = 1, for imaging in the forward scan direction only, and

n_S = 2, for imaging in both directions.

The active scan time t_A is given by Equation (4-4). However, in this case, the scan efficiency κ depends on the sensor design parameters; e.g., mirror turnaround time, value of n_S, and mirror inertia. The scan period T_M in this case is the time for the rocking mirror to do a forward scan and retrace to its initial position.

During each scan period an area on the ground is imaged. The extent imaged along the ground track at nadir (Figure 3) is

$$d_C = n_S n_D \alpha H \text{ [km]} . \tag{4-15}$$

Use of Equations (4-7), (4-9), and (4-15) results in

$$t_M = \frac{n_S n_D \alpha H}{B V_{SUB}} \text{ [sec]} . \tag{4-16}$$

Using Equations (4-4), (4-14), and (4-16) gives

$$t_D = \frac{\kappa \; n_D \alpha H}{n_E B V_{SUB}} \text{ [sec]} . \tag{4-17}$$

4.3 Linear Array

In this case, no scan mirror is used, and the number of angular resolution elements n_E is equal to the number of detectors in the cross-track direction. The dwell time for a linear array is, therefore,

$$t_D = \frac{\alpha H}{V_{SUB}} \text{ [sec]}, \tag{4-18}$$

and the field of view Θ is given by

$$\Theta = n_E \; \alpha \text{ [rad]} . \tag{4-19}$$

5. NOISE

The total sensor noise is composed of detector noise and system noise. The detector noise is composed of a number of different noises that depend on the material composition of the detector and whether it is a single detector or is used in an array.

The total sensor noise is given by

$$N_{TOT} = \left(N^2_{DET} + N^2_{SYS} \right)^{1/2} , \tag{5-1}$$

where N_{DET} = root-mean-square detector noise, and

N_{SYS} = root-mean-square system noise.

The following sections present a discussion of these various noise sources.

5.1 Visible and SWIR Detector Noise

Here we will describe the various types of noise encountered in visible and SWIR detectors.

5.1.1 Visible and SWIR Detector Noise Sources

5.1.1.1 Photon Noise

Photon noise or shot noise is due to the random arrival of photons at the detector. Because the incident photon flux follows a Poisson distribution, the photon noise is given by (Levi, 1968, p. 153)

$$N_P = (S')^{1/2} \ [e] , \tag{5-2}$$

where the signal S′ is the mean number of electrons produced by the photons arriving at the detector and is given by Equation (2-9).

5.1.1.2 Bulk Trap Noise

Bulk trap noise occurs in CCD focal plane arrays and arises from the random trapping and emission from interface or bulk states (Dereniak, 1984, p. 243) and is given by

$$N_{BT} = \left(M_g k_B T A_D n_{SS} \ \ell n \ 2 \right)^{1/2} \ [e], \tag{5-3}$$

where M_g = the number of gate transfers;

n_{SS} = the density of surface states;

A_D = the detector area;

k_B = Boltzmann's constant; and

T = Temperature [K].

Typical values of N_{BT} are:

- Surface Channel CCD–1000 electrons
- Buried Channel CCD–100 electrons.

5.1.1.3 Output Amplifier Noise

The output amplifier noise is associated with the amplifier that buffers the signal from the focal plane and is generally a metal oxide semiconductor field effect transistor (MOSFET) of a given transconductance. An expression that can be used to compute this noise is (Dereniak, 1984, p. 244)

$$N_{OA} = \left(\frac{8 C_o{}^2 k_B T \Delta f}{3 q^2 g_m} \right)^{1/2} \quad [e], \qquad (5\text{-}4)$$

where C_o = the output capacitance [μfarad];

Δf = the electrical bandwidth [Hz];

g_m = the transconductance of the MOSFET [mhos];

q = the charge of an electron [coul]; and

k_B = Boltzmann's constant.

5.1.1.4 Dark Current Noise

Dark current or thermal generation noise is associated with charge carriers that are thermally generated to bring the CCD potential well into thermal equilibrium. Dark current root-mean-square (rms) noise is given by (Honeywell, 1986, p. 5-26)

$$N_{DC} = \left(\frac{2 J_{DC} A_D t_I}{q} \right)^{1/2} \quad [e], \qquad (5\text{-}5)$$

where J_{DC} = dark current density at temperature T [a/cm^2];

A_D = detector area [cm^2];

t_I = integration time [sec]; and

q = electron charge [coul].

The dark current density J_{DC} is given by

$$J_{DC} = \alpha_M T^3 \exp\left(-\frac{qE_g}{\eta_M k_B T}\right) \tag{5-6a}$$

where E_g = silicon band gap = 1.12 eV;

k_B = Boltzmann's constant = 8.62×10^{-5} [eV/K];

T = temperature [K];

η_M = a material-dependent carrier recombination factor; for silicon η_M = 2; and

α_M = a material-dependent factor, typically $\alpha_M = 1.1 \times 10^{-6}$ [A/cm^3-K^3]

5.1.1.5 Johnson (Thermal) Noise

The thermal motion of electrons in a resistor gives rise to voltage fluctuations across the resistor leads. These fluctuations are known as Johnson or thermal noise. The noise current is given by (Dereniak, 1984, p. 39)

$$i_{rms} = \left(\frac{4k_B T\ \Delta f}{R}\right)^{1/2} \quad [A], \tag{5-7}$$

where Δf = the effective bandwidth of the circuit [Hz] and

R = the resistance [Ω].

It follows that the noise in electrons is given by

$$N_T = \frac{t_I}{R}\left(\frac{4k_B T\ \Delta f}{q}\right)^{1/2} \quad [e]\ . \tag{5-8}$$

5.1.1.6 Schottky Noise

Electrons in the semiconductor of an M-S (metal-semiconductor) junction may overcome the potential barrier to reach the metal and produce a noise current. The noise current is called Schottky barrier noise and is given by (Yang, 1978, p. 130)

$$I_o = A_D R_C T^2 \exp\left(-\frac{q\phi_m}{k_B T}\right) \ [A], \tag{5-9a}$$

where R_C = $4\pi qmk^2/h^3$ = Richardson's constant = 120 [A/cm^2-k^2];

A_D = detector area [cm];

$q\phi_m$ = work function = 0.0354 [eV], for PdSi:Si diodes;

k_B = Boltzmann's constant = 8.62 X 10^{-5} [eV/K];

T = temperature [K]; and

q = electron charge [coul].

The Schottky noise current can be converted to electrons and is given by

$$N_{DCS} = \left(\frac{I_o t_I}{q}\right)^{1/2} \quad [e]. \tag{5-9b}$$

5.1.1.7 Charge Transfer Noise

Charge transfer or transfer inefficiency noise is associated with CCD structures and occurs because of the random amount of charge lost by a signal upon transfer and the amount of charge introduced to a signal upon entering a well. The noise N_{CT} associated with a single well (Dereniak, 1984, p. 242) is given by

$$N_{CT} = \left(2\epsilon S'\right)^{1/2} \quad [e], \tag{5-10}$$

where ϵ = the transfer efficiency [nd].

If the number of detectors is n'_D, and the number of phases to transfer the charge is n_P, then the total number of wells is $n_P n'_D$. Hence the total charge transfer noise is given by

$$N_{CT} = \left(2\epsilon n'_D n_P S'\right)^{1/2} \quad [e] \ . \tag{5-11}$$

5.1.2 Visible and SWIR System Noise

5.1.2.1 Quantization Noise

The quantization noise N_Q is given by (Montgomery, 1978, p. B-1)

$$N_Q = \frac{S'_{SAT}}{12^{1/2}\ 2^Q} \quad [e], \tag{5-12}$$

where Q is the number of bits used in the analog-to-digital (A/D) converter. From Equation (2-9) one obtains for the visible and SWIR

$$S'_{SAT} = t_I A_D \eta \bar{E}'_{SAT} \Delta\lambda \quad [e], \tag{5-13}$$

where S'_{SAT} is the signal that would result if the detector were receiving the saturation irradiance. This is the flux that produces a signal level that just causes the A/D converter to saturate.

The saturation irradiance $\bar{E}'_{SAT}$ is given by

$$\bar{E}'_{SAT} = E'_M S_F \quad [\text{p/sec-cm}^2\text{-}\mu\text{m}], \tag{5-14}$$

where, from Equation (2-11), E'_M is given by

$$E'_M = \frac{\tau_o \pi}{4f^2_N} L'_M \quad [\text{p/sec-cm}^2\text{-}\mu\text{m}] . \tag{5-15}$$

When the saturation factor S_F is multiplied by the maximum expected scene irradiance E'_M at the detector, an irradiance $\bar{E}'_{SAT}$ will be produced that will just saturate the A/D converter.

5.1.2.2 Other System Noise

When system noises are from unknown sources, they are designated as other system noise.

5.2 Infrared Detector Noise

5.2.1 Infrared Detector Noise Sources

The detector noise is composed of two parts, photon noise and other noise. It is given by

$$N_{DET} = \left(N_P{}^2 + N_{OD}{}^2\right)^{1/2} \quad [e] . \tag{5-16}$$

We will calculate the photon noise N_P on the basis of a cold shielded and cold filtered detector. The other detector noise N_{OD}, will be estimated from laboratory values of D*. We will estimate the other detector noise from D* first.

5.2.1.1 Other Detector Noise

Consider the detector that will be used in the sensor (same area and electrical bandwidth), but with background temperature and viewing angles identical to those used in the laboratory measurement of D*.

The other detector noise N_{OD} is given by

$$N_{OD} = \left(NEE^2 - N_{PL}{}^2\right)^{1/2} \quad [e] \ . \tag{5-17}$$

The other detector noise N_{OD} is assumed to be independent of the level of cold shielding and cold filtering. The photon noise under laboratory conditions is

$$N_{PL} = \left(t_I F_L \ \pi \ \eta \ A_D \int_0^{\lambda_C} B'(T_{BGL}, \lambda) \, d\lambda\right)^{1/2} \quad [e], \tag{5-18}$$

where λ_C is the detector cutoff wavelength, T_{BGL} is the background temperature in the laboratory, $B'(T_{BGL}, \lambda)$ is defined by Equation (3-7), and F_L is the view factor in the laboratory ($F_L = 1$ when viewing 180°, or 2π steradians). In general

$$F_L = \sin^2\left(\frac{\phi_C}{2}\right) \quad [nd] \tag{5-19}$$

where ϕ_C is the full-cone view angle.

The detector noise equivalent power is given by

$$NEP = \frac{(A_D \ \Delta f)^{1/2}}{D^*} \quad [W] , \tag{5-20}$$

where A_D = detector are [cm^2]; and

D^* = the laboratory value of specific detectivity [$cm\text{-}Hz^{1/2}/W$].

The number of noise equivalent electrons NEE is given by

$$NEE = \frac{Rt_I}{q} NEP \quad [e] \tag{5-21}$$

and the effective noise bandwidth is given by

$$\Delta f = \frac{\beta}{2t_I} \quad [kHz], \tag{5-22}$$

where β is the ratio of noise bandwidth to information bandwidth, and t_I is the integration time given by Equation (2-8).

5.2.1.2 Photon Noise (Infrared)

The photon noise is given by (Levi, 1968, p. 153)

$$N_P = (\tau')^{1/2} \quad [e], \tag{5-23}$$

where the total number of electrons produced by the scene and background is given by

$$\tau' = t_I A_D \eta \left[\int_{\lambda_1}^{\lambda_2} E'(\lambda)\, d\lambda + \int_{\lambda'_1}^{\lambda'_2} E'_{BG}(\lambda)\, d\lambda \right] \quad [e], \tag{5-24}$$

where λ_1 to λ_2 is the spectral bandpass of the scene photon spectral irradiance $E'(\lambda)$, which is given by Equation (2-11), and λ'_1 to λ'_2 is the spectral bandpass of the background photon spectral irradiance $E'_{BG}(\lambda)$, which is governed by the cold filter.

The background spectral irradiance $E'_{BG}(\lambda)$ is given by

$$E'_{BG}(\lambda) = \left[\Omega\, \epsilon_o + (\Omega_{BG} - \Omega)\, \tau_{CF} \right] B'(\lambda, T_{BG}) \quad [\text{p/sec-cm}^2\text{-}\mu\text{m}] \tag{5-25}$$

and the emissivity of the optics is given by

$$\epsilon_o = 1 - \tau_o \quad [\text{nd}], \tag{5-26}$$

where $B'(\lambda, T_{BG})$ = the background spectral photon radiance, [p/sec-cm^2-sr-μm] obtained from Equation (3-7);

T_{BG} = the background temperature [K] of any radiant energy source other than the ground resolution element; and

τ_{CF} = optical transmission [nd] of the cold filter.

The effective solid angle Ω (Figure 5) through which the detector receives energy from the ground resolution element is given by

$$\Omega = \frac{\pi}{4f^2_N} \quad [\text{sr}]\ . \tag{5-27}$$

The background effective solid angle Ω_{BG} includes the effective solid angle Ω plus a little more for tolerance purposes. Ideally, they would be identical.

Solid Angles

$\Omega' = 2\pi(1-\cos\theta)$
$\Omega'_{BG} = 2\pi(1-\cos\theta_{BG})$

Effective Solid Angles

$\Omega = \pi\sin^2(\theta) = \frac{\pi}{4f_N^2}$

$\Omega_{BG} = \pi\sin^2(\theta_{BG})$

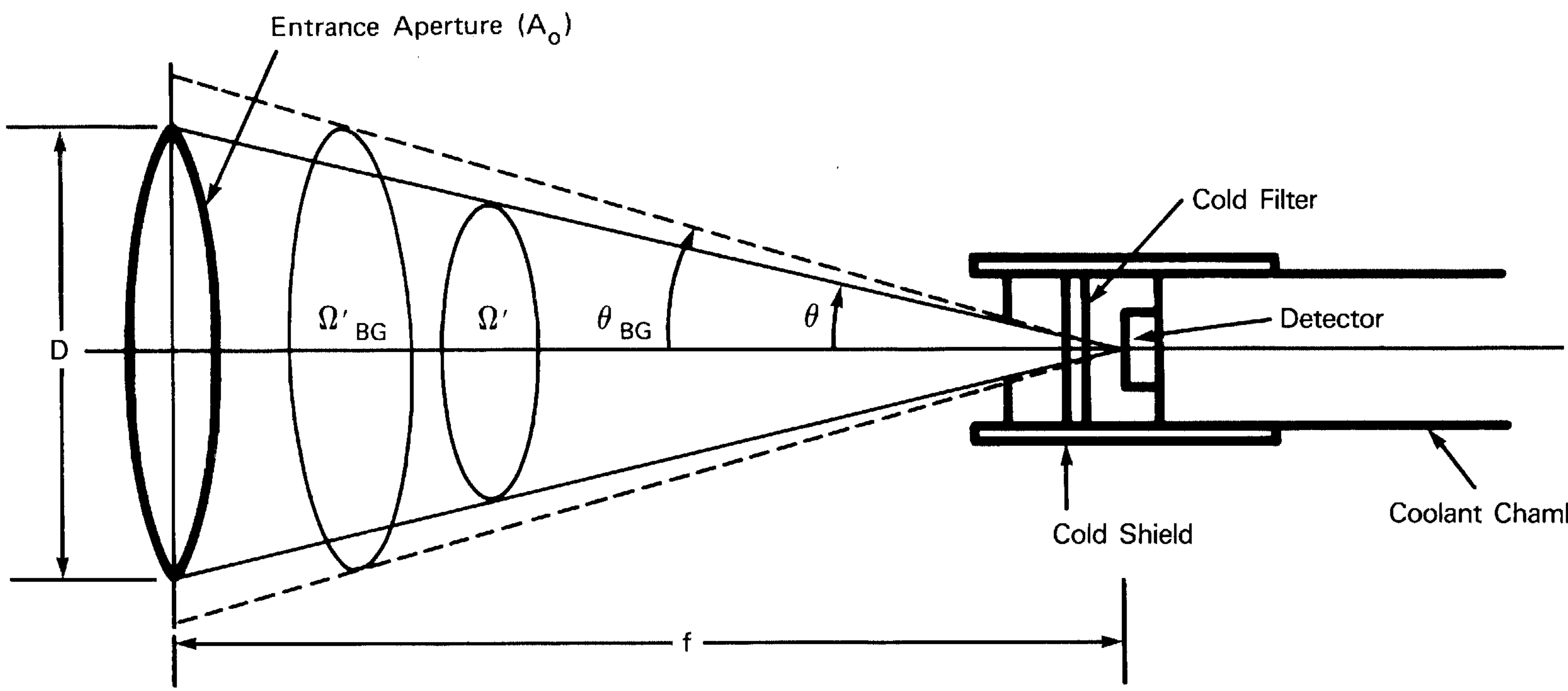

A_o	= Area of sensor entrance aperture (cm^2)	Ω	= Optics effective solid angle (sr)
D	= Diameter of sensor entrance aperture (cm)	Ω_{BG}	= Background effective solid angle (sr)
f	= Focal length (cm)	Ω'	= Optics solid angle (sr)
θ	= Optics half-cone angle (deg)	Ω'_{BG}	= Background solid angle (sr)
θ_{BG}	= Background half-cone angle (deg)		

Figure 5. Background Viewing Geometry

The effective solid angle of the background Ω_{BG} is given by

$$\Omega_{BG} = \pi F_S \quad [sr], \tag{5-28}$$

where the view factor F_S is defined as

F_S = F_C for a cold shielded detector viewing the scene through a circular aperture (Appendix D), and

F_S = F_A for a detector array surrounded by a cold fence (Appendix E).

It follows that:

$$F_C = \sin^2 \left[\frac{\theta_{BG}}{2} \right] \quad [sr], \tag{5-29}$$

where θ_{BG} is the full-cone angle [deg] of the background.

From Equation (5-20) one can write

$$D^*_S = \frac{[A_D \ \Delta f]^{1/2}}{NEP} \qquad [cm\text{-}Hz^{1/2}/W] \tag{5-30}$$

and

$$NEP = \frac{q}{R(\lambda)\ t_I} \left[N_P^2 + N_{OD}^2 \right]^{1/2} \quad [W] \ . \tag{5-31}$$

Substituting Equation (5-31) into Equation (5-30) and setting $N_{OD} = 0$ yields

$$D^*_{BLIP}(\lambda) = \frac{R(\lambda) t_I \left(A_D \ \Delta f\right)^{1/2}}{q N_P} \qquad [cm\text{-}Hz^{1/2}/W] \tag{5-32}$$

where D^*_{BLIP} is the background-limited photon (BLIP) value of D^*.

Substituting Equations (2-3), (5-21), (5-23), and (5-24) into Equation (5-32) gives

$$D^*_{BLIP}(\lambda) = \frac{\lambda}{h\ c} \left(\frac{\eta}{2} \right)^{1/2} \left(\int_{\lambda_1}^{\lambda_2} E'(\lambda)\ d\lambda + \int_{\lambda'_1}^{\lambda'_2} E'_{BG}\ d\lambda \right)^{-1/2} \quad [cm\text{-}Hz^{1/2}/W] \ . \tag{5-33}$$

Equation (5-33) includes only the photon noise and is for a photovoltaic detector. For a photoconductive detector there is an additional term due to generation-recombination noise, and it reduces D^*_{BLIP} by a factor of $(2)^{1/2}$.

5.2.2 Infrared System Noise

5.2.2.1 Quantization Noise

The quantization noise is given by (Montgomery, 1978, p. B-1)

$$N_Q = \frac{S'_{SAT}}{(12)^{1/2}\, 2^Q} \quad [e], \tag{5-34}$$

where Q is the number of bits used in the A/D converter.

The infrared saturation signal is given by

$$S'_{SAT} = t_i A_D \eta \int_{\lambda_1}^{\lambda_2} E'_{SAT}(\lambda)\, d\lambda \quad [e], \tag{5-35}$$

where the infrared saturation spectral photon irradiance $E'_{SAT}(\lambda)$ is given by (see Appendix A)

$$E'_{SAT}(\lambda) = \frac{\tau_o \pi}{4f_N^2} L'_{SAT}(\lambda) \quad [\text{p/sec-cm}^2\text{-}\mu\text{m}] \tag{5-36}$$

and where the infrared saturation radiance $L'_{SAT}(\lambda)$ is the appropriate value to just saturate the A/D converter.

5.2.2.2 Other Infrared System Noise

When the system noises are from unknown sources, they are designated as other system noise.

6. FIGURES OF MERIT

One important figure of merit that we will discuss here is the signal-to-noise ratio SNR, which is easily obtained by using the results of Section 2 for the signal S′ and Section 5 for the noise N_{TOT}. We will also discuss a figure of merit used in the visible and SWIR bands, the Noise Equivalent Delta Reflectance (NE$\Delta\rho$), and for the infrared we shall discuss the Noise Equivalent Delta Temperature (NEΔT).

6.1 Noise Equivalent Delta Reflectance

When visible sensors are assessed with respect to surface observations such as reflectance, the SNR is not always a convenient figure of merit. Users of space or airborne remote sensor data are frequently concerned with the characterization of ground targets through the measurement of variations in target reflectance. Because the variations of interest are often small in magnitude and are difficult to measure precisely, there is considerable interest in the definition and measurement of the capability of the sensor to respond to small reflectance changes. This capability, related to sensitivity, is often described in terms of Noise Equivalent Delta Reflectance (NE$\Delta\rho$), which is the minimum detectable variation in reflectance, and is sometimes preferred by the science user community over the spatial resolution of the system.

For the visible and SWIR bands, NE$\Delta\rho$ is the amount by which ρ would need to change to cause the signal to change by an amount equal to the noise, or it is the smallest change in reflectance between two adjacent surface elements that can be resolved by the sensor. In this section we compute NE$\Delta\rho$ from the SNR.

The figure of merit NE$\Delta\rho$ is given by

$$NE\Delta\rho = \frac{L}{\left(\frac{S}{N}\right)\left(\frac{dL}{d\rho}\right)} = \frac{\gamma}{\frac{S}{N}} \quad [nd], \qquad (6\text{-}1)$$

where γ (see Appendix F) is

$$\gamma = \frac{\gamma_0}{\tau_{AN}^{(\sec\phi' - 1)}} \quad [nd] \qquad (6\text{-}2)$$

and where

$$\gamma_o = \frac{\rho}{1 - \dfrac{L_A^N}{L^N}} \quad [\text{nd}] \; . \tag{6-3}$$

Also, ϕ' is the angle between the line of sight and the surface normal (see Figure 6) and L_A^N and L^N are the atmospheric and scene radiances respectively, from the tables in Appendix B.

The atmospheric optical transmission in the nadir direction τ_{AN} is given by

$$\tau_{AN} = e^{-\delta_{TN}} \quad [\text{nd}], \tag{6-4}$$

where the total nadir optical thickness δ_{TN} is obtained from the tables in Appendix B.

6.2 Noise Equivalent Delta Temperature

For the infrared bands NEΔT is given by

$$\text{NE}\Delta\text{T} = \frac{L'}{\tau_A \left(\dfrac{S}{N}\right)\left(\dfrac{dL'_S}{dT_S}\right)} \quad [\text{K}] \tag{6-5}$$

where L' = the scene photon radiance [p/sec–cm^2–sr],

τ_A = atmospheric transmission [nd],

S = signal [e],

N = noise [e], and

dL'_S/dT_S = the differential change in surface radiance with respect to surface temperature [p/sec–cm^2–sr–K].

(See Appendix G for a detailed derivation.)

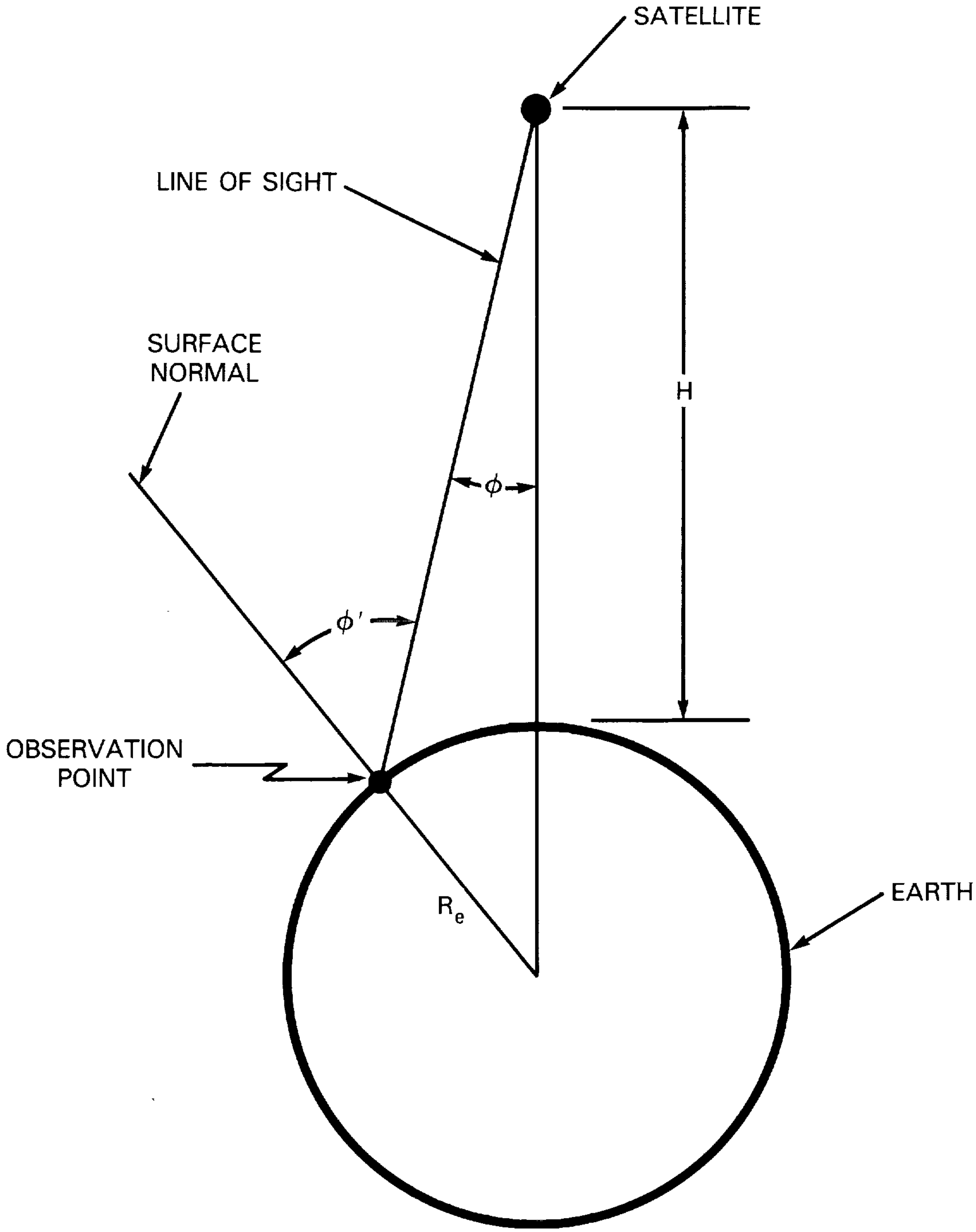

$$\phi' = \sin^{-1}\left[\left(1 + \frac{H}{R_e}\right)\sin\phi\right]$$

ϕ = Sensor view angle (deg)
ϕ' = Angle between line of sight and the surface normal (deg)
H = Height
R_e = Radius of Earth

Figure 6. Satellite/Scene Viewing Geometry

7. MODULATION TRANSFER FUNCTION (MTF)

If the sensor were to scan a very low spatial frequency (sinusoidal variation in radiance) an amplitude variation $\Delta S(0)$ in signal would result. At spatial frequency k [cycles/mm] an amplitude variation of $\Delta S(k)$ would be obtained. The ratio of $\Delta S(k)$ to $\Delta S(0)$ is the Modulation Transfer Function (MTF) of the sensor; i.e.,

$$MTF = \frac{\Delta S(k)}{\Delta S(0)} \quad [nd] \tag{7-1}$$

7.1 Total MTF

For a linear system, the total modulation transfer function is the product of the modulation transfer functions of the individual elements of the system. There are many different MTFs associated with a sensor system, which typically might include:

- MTF_{OA} = Optical Aperture MTF
- MTF_{DA} = Detector Aperture MTF
- MTF_{SM} = Satellite Motion MTF
- MTF_{CD} = Charge Diffusion MTF
- MTF_{CT} = Charge Transfer MTF
- MTF_{SJ} = Satellite Jitter MTF.

The total or system MTF is the product of the component MTFs; i.e.,

$$MTF = MTF_{OA} \cdot MTF_{DA} \cdot MTF_{SM} \cdot MTF_{CD} \cdot MTF_{CT}$$

7.2 Component MTFs

In this section we list the MTF equations and their reference sources.

7.2.1 Optical Aperture MTF

The diffraction MTF is given by (O'Neill, 1955 and 1956)

$$MTF_{OA} = \frac{A_m + B_m + C_m}{(1 - \beta^2)} \, , \tag{7-2}$$

where

$$A_m = \frac{2}{\pi} \left\{ \mathrm{Cos}^{-1} \left(\frac{\Lambda}{2}\right) - \left(\frac{\Lambda}{2}\right) \left[1 - \left(\frac{\Lambda}{2}\right)^2 \right]^{1/2} \right\} \qquad \text{for } 0 \leqslant \frac{\Lambda}{2} \leqslant 1 \qquad (7\text{-}3)$$

and

$$A_m = 0 \qquad \text{for } \frac{\Lambda}{2} > 1, \qquad (7\text{-}4)$$

where

$$B_m = \frac{2\beta^2}{\pi} \left\{ \mathrm{Cos}^{-1} \left(\frac{\Lambda}{2\beta}\right) - \left(\frac{\Lambda}{2\beta}\right) \left[1 - \left(\frac{\Lambda}{2\beta}\right)^2 \right]^{1/2} \right\} \qquad \text{for } 0 \leqslant \frac{\Lambda}{2\beta} \leqslant 1 \qquad (7\text{-}5)$$

and

$$B_m = 0 \qquad \text{for } \frac{\Lambda}{2\beta} > 1 \qquad (7\text{-}6)$$

and where

$$C_m = -2\beta^2 \qquad \text{for } 0 < \frac{\Lambda}{2} \leqslant \frac{(1 - \beta)}{2} \qquad (7\text{-}7)$$

$$C_m = -2\beta^2 + \frac{2\beta}{\pi} \mathrm{Sin}\psi + \left(\frac{1 + \beta^2}{\pi}\right) \psi$$
$$-2 \left(\frac{1 - \beta^2}{\pi}\right) \mathrm{Tan}^{-1} \left[\left(\frac{1 + \beta}{1 - \beta}\right) \mathrm{Tan} \frac{\psi}{2} \right]$$
$$\text{for } \frac{1 - \beta}{2} \leqslant \frac{\Lambda}{2} \leqslant \frac{1 + \beta}{2} \qquad (7\text{-}8)$$

and

$$C_m = 0 \qquad \text{for } \frac{\Lambda}{2} > \frac{1 + \beta}{2}, \qquad (7\text{-}9)$$

and ψ is given by

$$\psi = \mathrm{Cos}^{-1} \left(\frac{1 + \beta^2 - \Lambda^2}{2\beta}\right) \qquad (7\text{-}10)$$

with

$$\Lambda = \frac{k}{k_0} \qquad (7\text{-}11)$$

where k is the spatial frequency [cycles/mm] measured in the image plane and

$$k_0 = \frac{1}{2\lambda f_N} \quad [\text{cycles/mm}] \; . \tag{7-12}$$

The modulation transfer function $MTF_{OA} = 0$ for $\Lambda = 2$ at the cutoff frequency when $k = k_C$, where

$$k_C = 2\,k_0 \quad [\text{cycles/mm}], \tag{7-13}$$

and where

$$f_N = \frac{f}{D} \quad [\text{nd}] \; . \tag{7-14}$$

where λ is the wavelength, f is the focal length of the optics, and D is the diameter of the optics; and

$$\beta = \frac{D_o}{D} \quad [\text{nd}] \tag{7-15}$$

where D_o is the diameter of any obscuration.

Note that the quantity k_0 given in Equation (7-12) is not defined in O'Neill's paper but must be defined this way to be consistent with his Figure 3 in which the MTF goes to zero at $\Lambda = 2.0$.

7.2.2 Detector Aperture MTF

The detector aperture MTF is given by (Jensen, 1968, p. 27)

$$MTF_{DA} = \left| \frac{\sin(\pi k d_S)}{\pi k d_S} \right| \tag{7-16}$$

where d_S = the detector width [mm], and

k = spatial frequency in the image plane [cycles/mm].

7.2.3 Satellite Motion MTF

The MTF due to linear image motion is given by (Jensen, 1968, p. 117)

$$MTF_{SM} = \left| \frac{\sin(\pi k V_I t_I)}{\pi k\, V_I t_I} \right| \tag{7-17}$$

where the image velocity V_I is given by

$$V_I = \frac{f V_{SUB}}{H} \quad [\text{km/sec}], \tag{7-18}$$

where V_{SUB} = the subsatellite point velocity [km/sec];

k = spatial frequency in the image plane [cycles/mm]; and

t_I = integration time [sec].

7.2.4 Charge Diffusion MTF

The charge diffusion MTF is given by (Jespers, 1975, p. 519)

$$MTF_{CD} = \frac{1 - \dfrac{\exp - \alpha_a d}{1 + \alpha_a L}}{\dfrac{\exp - \alpha_a d}{1 + \alpha_a L_o}} \tag{7-19}$$

where d = photodetector depletion region depth (typical value = 5 μm).

The silicon absorption coefficient α_a is a function of wavelength and temperature and is given by

$$\alpha_a = 10^z \quad [\mathrm{cm}^{-1}] \tag{7-20}$$

where, after curve fitting to Jespers' Figure 25 for silicon, we have

$$\begin{aligned} z = {} & 2.897652 - 4.044143\ (\lambda - 0.82) - 5.219219\ (\lambda - 0.82)^2 \\ & - 3.828495\ (\lambda - 0.82)^3 + 22.16724\ (\lambda - 0.82)^4\ , \end{aligned} \tag{7-21}$$

where λ = wavelength [μm],

L_0 = diffusion length (typical value = 50 μm),

and where

$$L = \left[\frac{L_0{}^2}{1 + (2\pi k L_0)^2} \right]^{1/2} . \tag{7-22}$$

7.2.5 Charge Transfer MTF

The MTF due to inefficiency in charge transfer in a CCD detector is given by (Jespers, 1976, p. 520)

$$MTF_{CT} = e^{-M_{CT}\,\epsilon \left[1 - \cos\left(\frac{\pi k}{k_{max}}\right)\right]} \tag{7-23}$$

where ϵ is the charge transfer inefficiency and where the number of charge transfers M_{CT} is given by

$$M_{CT} = m_S m_P \ , \tag{7-24}$$

where m_S = the number of stages, detectors, or picture elements, and

m_P = the number of clock phases for readout.

The Nyquist spatial frequency k_{max} is given by

$$k_{max} = \frac{1}{2P_D} \ , \tag{7-25}$$

where P_D is the detector pitch.

7.2.6 Satellite Jitter MTF

The satellite jitter MTF is given by (Jensen, 1968, p. 124)

$$MTF_{SJ} = J_0(2\pi k f \Theta_M) \tag{7-26}$$

where Θ_M = maximum satellite angular movement [rad],

J_0 = zeroth order Bessel function, and

f = focal length (mm).

8. REFERENCES

Dereniak, E. L. and D. G. Crowe, "Optical Radiation Detectors," John Wiley and Sons, New York, 1984.

Dwight, H. B., "Tables of Integrals and Other Mathematical Data," The MacMillan Company, New York, 1961.

Goldberg, L., Unpublished Notes, 1985.

Honeywell Electro-Optics Operations, Multispectral Linear Array Instrument Definition Study, Final Report, 1986, pp. 5-26.

Hudson, R. D., "Infrared Systems Engineering," John Wiley and Sons, New York, 1969.

Jespers, P. G., F. Van De Wiele and M. H. White, "Solid State Imaging," Noordhoff, The Netherlands, 1976.

Jensen, N., "Optical and Photographic Reconnaissance Systems," John Wiley and Sons, New York, 1968.

Levi, L., "Applied Optics: A Guide to Modern Optical System Design," John Wiley and Sons, New York, 1968.

Montgomery, H. and E. Schell, "The Effects of Quantization on Signal Processing," NASA Technical Memorandum 78092, 1978.

O'Neill, E. L., Journal of the Optical Society of America, 46, 285, (1956).

O'Neill, E. L., Journal of the Optical Society of America, (1955).

Wolfe, W. L., G. J. Zeiss, "The Infrared Handbook", Office of Naval Research, Department of the Navy, Washington, D.C. 1978.

Yang, E. S., "Fundamentals of Semiconductor Devices," McGraw-Hill, New York, 1978, p. 130.

APPENDIX A

DETECTOR IRRADIANCE

The objective of this appendix is to show the relationship between the scene spectral radiance and the irradiance on the detector.

When a sensor images an area on the surface of the Earth called the instantaneous field of view (IFOV), it also receives energy from the intervening atmosphere. The scene spectral radiance $L(\lambda)$ [W/cm^2-sr-μm] is defined as the combined spectral radiance from the atmosphere and the IFOV area A_I as viewed from the sensor. The power that the area A_I and the intervening atmosphere radiate through the solid angle Ω_o into the sensor entrance aperture and into the detector is then

$$\Phi = \int_{\lambda_1}^{\lambda_2} d\phi(\lambda) \quad [W] \tag{A-1}$$

where

$$d\phi(\lambda) = \tau_o \Omega_o A_I L(\lambda)\, d\lambda \quad [W] \tag{A-2}$$

and where τ_o = the sensor optical transmission. However, by definition, for a detector of area A_D, Equation (A-2) may also be written in terms of the detector spectral irradiance $E(\lambda)$ [W/cm^2-μm] as

$$d\phi(\lambda) = A_D E(\lambda)\, d\lambda \quad [W] \tag{A-3}$$

By comparing Equations (A-2) and (A-3), one can express the scene spectral irradiance $E(\lambda)$ in terms of the scene spectral radiance $L(\lambda)$ and sensor design-related parameters A_D, A_I, and Ω_o as

$$E(\lambda) = \frac{\tau_o \Omega_o A_I}{A_D} L(\lambda) \quad [W/cm^2\text{-}\mu m) . \tag{A-4}$$

Now, from Figure A-1,

$$A_I = \alpha^2 H^2, \tag{A-5}$$

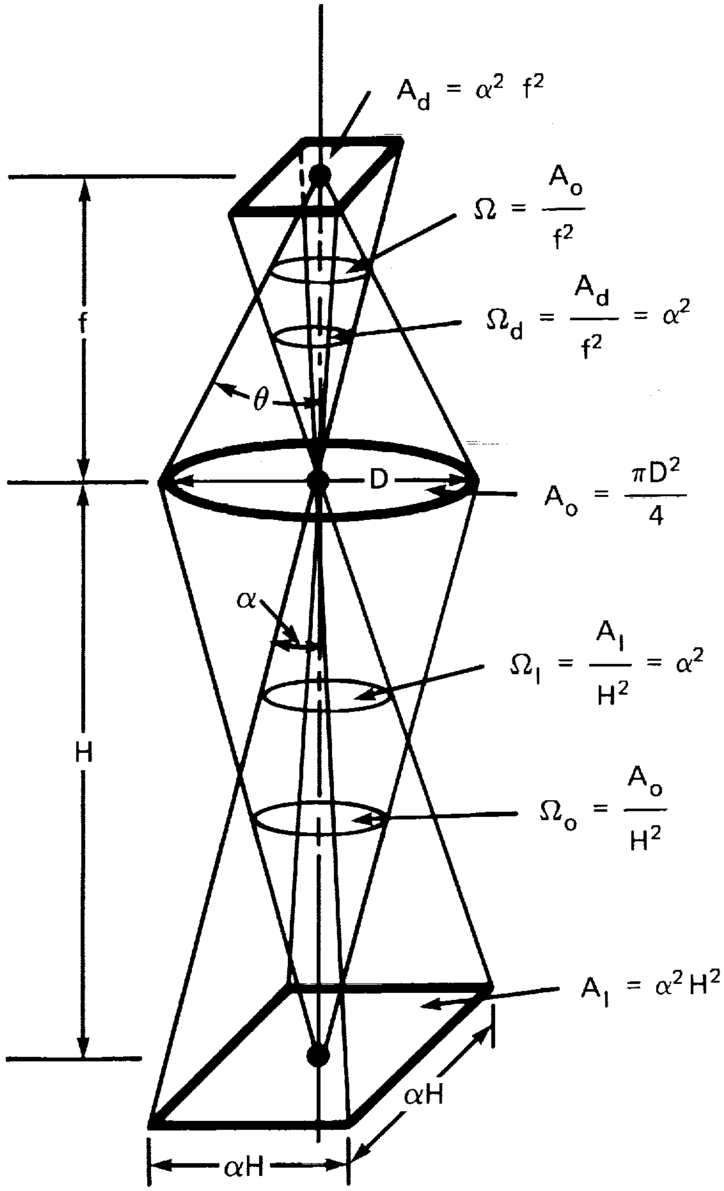

A_d = Detector area (μm^2)
A_o = Area of sensor entrance aperture (cm^2)
A_I = Area of ground resolution element (cm^2)
D = Diameter of sensor entrance aperture (cm)
f = Effective focal length (cm)
H = Satellite height (km)
α = Instantaneous angular FOV (as in previous figs) (rad)
θ = Half-cone angle of optics (deg)
Ω = The effective solid angle through which the detector receives energy (sr)
Ω_o = Solid angle subtended by the sensor entrance aperture at the ground resolution element (sr)
Ω_I = Solid angle subtended by the ground resolution element at the sensor entrance aperture (sr)
Ω_d = Solid angle subtended by the detector at the entrance aperture (sr)

Figure A-1. Radiometric Geometry

where α = the sensor instantaneous field of view (IFOV), and

H = the distance from the satellite to the area A_I.

Also, for a square detector

$$A_D = \alpha^2 f^2, \tag{A-6}$$

where f is the sensor optics effective focal length, which represents the optical path length and is approximately equal to the geometric focal length for small optical convergence angles (<10°), and

$$\Omega_o = \frac{A_o}{H^2} = \frac{\pi D^2}{4H^2}, \tag{A-7}$$

where D = aperture diameter of the sensor.

Using Equations (A-5), (A-6) and (A-7), one can write

$$\frac{A_I \Omega_o}{A_D} = \frac{\pi}{4f^2_N} \tag{A-8}$$

where the sensor optics f-number f_N is given by

$$f_N = \frac{f}{D}. \tag{A-9}$$

The half-cone angle θ of the optics is given by

$$\sin \theta = \frac{D}{2f}. \tag{A-10}$$

It is also given by

$$\tan \theta = \frac{D}{2f'}. \tag{A-11}$$

The f-number f_N is related to the approximate f-number $\left(\frac{f'}{D}\right)$ by the expression

$$f_N = \left(\frac{f'}{D}\right) \left[1 + \left(\frac{1}{2 \frac{f'}{D}} \right)^2 \right]^{1/2} \tag{A-12}$$

Substituting Equation (A-8) into Equation (A-4) (See Figure A-2) gives

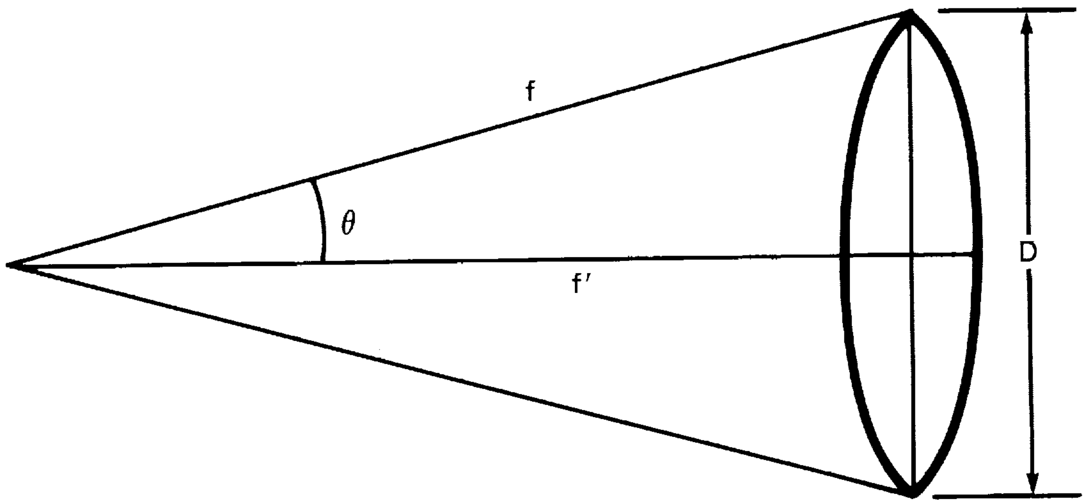

f_N	Δ(%)
1	13.4
1.1	10.9
1.2	9.1
1.3	7.7
1.4	6.6
1.5	5.7
2	3.2
3	1.9
4	0.8
5	0.5

$$f_N = \text{F-NUMBER}$$

$$= \frac{f}{D} = \frac{1}{2 \sin \theta}$$

$$= \frac{f'}{D}\left[1 + \left(\frac{1}{2\,\frac{f'}{D}}\right)^2\right]^{1/2}$$

$$\Delta = \left(f_N - \frac{f'}{D}\right) \Big/ 100\, f_N$$

Figure A-2. Comparison of f_N and f'/D

$$E(\lambda) = \frac{\pi\tau_o}{4f^2_N} L(\lambda) \qquad [W/cm^2\text{-}\mu m] \ . \tag{A-13}$$

REFERENCES

Fraser, Unpublished Memorandum, 1981.

Mattoo, S., "Tabulation of the Atmospheric Effect on Spectral Signature of the Surface," Unpublished NASA Technical Report, 1984.

APPENDIX B

COMPUTED EARTH ATMOSPHERE RADIANCES

With the permission of the authors, the following discussion has been taken from a NASA unpublished report (Mattoo, 1984) and a memorandum (Fraser, 1981).

The computed radiances at the top of the Earth-atmosphere system are tabulated for 15 wavelengths. The computations are made for plane-parallel models of the Earth-atmosphere system; that is, the optical properties of the models do not vary in a horizontal plane. However, the vertical profiles of the concentrations of the atmospheric constituents are arbitrary, but realistic. The ground reflects light according to Lambert's law, which implies that the radiance of the reflected light is constant, independent of direction.

Only one atmospheric model is used, and it contains the standard dry gas and the gases that absorb in the spectral bands of interest. The variable trace gases are 316 Dobson units of O_3 and 2.5 cm of H_2O. The model also contains particulates, but not liquid or ice clouds.

The average normal optical thickness of each constituent is given for each spectral band in Table B-1. The total nadir optical thickness (δ_{TN}) at a wavelength equals the sum of the optical thicknesses of the constituents:

$$\delta_{TN} = \delta_R + \delta_G + \delta_A \ , \qquad \text{(B-1)}$$

where δ_R = the scattering optical thickness (Rayleigh) of the dry atmosphere,

δ_A = the optical thickness of the aerosols (particulates), and

δ_G = the optical thickness of the absorbing gases.

The total optical transmission τ for the direct sunlight is given by

$$\tau = \frac{E_{\lambda s}}{E_{\lambda o}} = \exp(-\delta_{TN} \sec \theta_z) \qquad \text{(B-2)}$$

where $E_{\lambda s}$ and $E_{\lambda o}$ are the spectral irradiance of the direct sunlight at sea level and above the atmos-

Table B-1. Optical Thicknesses for Scattering by Molecules (δ_R), Absorption by Gases (δ_G), and Scattering from Aerosols (δ_A)

λ	0.4	0.44	0.48	0.52	0.56
δ_R	0.3637	0.2451	0.1713	0.1234	0.0912
δ_G	0.0000	0.0007	0.0048	0.0151	0.0296
δ_A	0.3600	0.3273	0.3000	0.2796	0.2571
δ_{TN}	0.7237	0.5731	0.4761	0.4181	0.3779
λ	0.62	0.66	0.70	0.74	0.82
δ_R	0.0603	0.0468	0.0368	0.0294	0.0195
δ_G	0.0325	0.0169	0.0135	0.0145	0.0560
δ_A	0.2370	0.2228	0.2087	0.1988	0.1794
δ_{TN}	0.3298	0.2865	0.2590	0.2427	0.2549
λ	0.88	1.05	1.25	1.60	2.20
δ_R	0.0147	0.0072	0.0036	0.0013	0.0004
δ_G	0.0039	0.0000	0.0092	0.0066	0.0608
δ_A	0.1694	0.1420	0.1193	0.0932	0.0682
δ_{TN}	0.1880	0.1492	0.1321	0.1011	0.1294

phere, respectively, and θ_z is the solar zenith angle. The values of $E_{\lambda o}$ are given in Table B-2. The quantity $E_{\lambda o}$ is the solar irradiance on a square centimeter of surface perpendicular to the solar rays.

The aerosols (particulates) are assigned properties of those occurring in continential regions. The size distribution function (n) of the particle radius (r), which is the number of particles per cubic centimeter of air per micrometer of radius, decreases very rapidly with increasing radius:

$$n \sim r^{-4} \; . \tag{B-3}$$

The index of refraction of the particulates is m = 1.4300 - 0.0035i. The nadir radiances of the model are not sensitive to the vertical profile of the particulate concentration. Here, a realistic profile with a high concentration near the ground is assumed.

The computations are made with a computer code developed by Dr. J. V. Dave of IBM as modified by R. S. Fraser of NASA. The equation of radiative transfer is solved numerically by a procedure that iteratively accounts for successive scatterings of light from the atmosphere and the ground. The polarization characteristics are not accounted for, and as a result, the computed radiances are in error by a few percent.

The input parameters for the computations include the model parameters: the vertical profiles of the concentrations of the gases and aerosols (particulates), the scattering and absorption optical thickness, the gaseous absorption coefficients, and 10 values of the surface reflectance ρ. The volume extinction, scattering and absorption coefficients and scattering phase function of the particulates are computed according to the Mie theory by a separate code, and are part of the input.

The nadir spectral radiance at the top of the atmosphere L^N can be expressed as follows:

$$L^N = L_S \, e^{-\delta_{TN}} + L_A^N \; , \tag{B-4}$$

where the first term on the right-hand side of the equation gives the radiance at the surface (ground) L_S (assumed to be Lambertian) attenuated by the atmosphere; the second term gives the radiance of just the atmosphere L_A^N, or path radiance. The radiances L^N and L_A^N are given in Table B-2, where

λ = the center wavelength [mm],

θ_z = the solar zenith angle [rad],

ρ = the surface reflectance [nd],

δ_{TN} = the total optical thickness [nd],

$E_{\lambda o}$ = the solar spectral irradiance [mW/cm^2-μm],

L^N = the total nadir spectral radiance [mW/cm^2-sr-μm] and

L_A^N = the atmospheric path spectral radiance [mW/cm^2-sr-μm].

Table B-2. Reflected Solar Spectral Radiance

$\lambda = 0.400\ \mu m$, $E_{\lambda o} = 165.400\ mW/cm^2\text{-}\mu m$, $\delta_{TN} = 0.72$

ρ	0.00		0.01		0.05		0.10		0.20	
θ_z	L^N	L_A^N	L^N	L_A^N	L^N	L_A^N	L^N	L_A^N	L^N	L_A^N
0.0	7.894	7.894	8.230	8.025	9.594	8.569	11.341	9.291	14.987	10.885
10.0	7.757	7.757	8.091	7.890	9.447	8.441	11.183	9.173	14.806	10.785
20.0	7.531	7.531	7.844	7.655	9.115	8.167	10.743	8.847	14.140	10.347
30.0	7.042	7.042	7.327	7.156	8.484	7.627	9.966	8.254	13.058	9.634
40.0	6.473	6.473	6.717	6.570	7.705	6.973	8.970	7.507	11.611	8.683
50.0	5.847	5.847	6.041	5.924	6.826	6.244	7.832	6.669	9.931	7.604
60.0	5.126	5.126	5.263	5.181	5.821	5.407	6.535	5.707	8.024	6.369
70.0	4.152	4.152	4.233	4.185	4.563	4.320	4.985	4.499	5.865	4.893
80.0	2.552	2.552	2.584	2.565	2.710	2.615	2.873	2.681	3.211	2.829

ρ	0.30		0.40		0.50		0.75		1.00	
θ_z	L^N	L_A^N	L^N	L_A^N	L^N	L_A^N	L^N	L_A^N	L^N	L_A^N
0.0	18.848	12.695	22.944	14.741	27.298	17.045	39.484	24.104	53.944	33.437
10.0	18.643	12.612	22.714	14.672	27.041	16.989	39.152	24.073	53.522	33.418
20.0	17.739	12.048	21.556	13.969	25.614	16.130	36.970	22.744	50.445	31.478
30.0	16.333	11.197	19.809	12.960	23.502	14.942	33.840	20.999	46.106	28.985
40.0	14.409	10.017	17.376	11.520	20.531	13.211	29.359	18.379	39.835	25.195
50.0	12.155	8.665	14.514	9.860	17.021	11.204	24.038	15.313	32.365	20.732
60.0	9.602	7.120	11.276	7.967	13.056	8.918	18.036	11.830	23.945	15.670
70.0	6.797	5.340	7.787	5.843	8.838	6.409	11.781	8.136	15.273	10.414
80.0	3.570	2.996	3.950	3.186	4.355	3.399	5.487	4.053	6.830	4.918

Table B-2. Reflected Solar Spectral Radiance (Continued)

$\lambda = 0.440\ \mu m$, $E_{\lambda o} = 177.300\ mW/cm^2\text{-}\mu m$, $\delta_{TN} = 0.57$

ρ	0.00		0.01		0.05		0.10		0.20	
θ_z	L^N	L_A^N	L^N	L_A^N	L^N	L_A^N	L^N	L_A^N	L^N	L_A^N
0.0	6.124	6.124	6.534	6.263	8.191	6.838	10.305	7.598	14.677	9.263
10.0	6.006	6.006	6.408	6.142	8.033	6.705	10.106	7.450	14.395	9.083
20.0	5.839	5.839	6.219	5.968	7.756	6.501	9.717	7.205	13.772	8.750
30.0	5.442	5.442	5.786	5.559	7.178	6.040	8.953	6.676	12.624	8.071
40.0	4.997	4.997	5.294	5.098	6.495	5.516	8.027	6.068	11.196	7.278
50.0	4.548	4.548	4.786	4.629	5.750	4.965	6.980	5.409	9.523	6.381
60.0	4.057	4.057	4.230	4.116	4.926	4.360	5.815	4.683	7.653	5.389
70.0	3.437	3.437	3.536	3.469	3.939	3.602	4.452	3.779	5.515	4.167
80.0	2.269	2.269	2.307	2.280	2.460	2.329	2.656	2.393	3.062	2.536

ρ	0.30		0.40		0.50		0.75		1.00	
θ_z	L^N	L_A^N	L^N	L_A^N	L^N	L_A^N	L^N	L_A^N	L^N	L_A^N
0.0	19.254	11.133	24.051	13.223	29.084	15.549	42.823	22.520	58.490	31.420
10.0	18.884	10.917	23.590	12.967	28.527	15.248	42.003	22.084	57.371	30.813
20.0	18.018	10.484	22.469	12.423	27.138	14.581	39.882	21.047	54.416	29.302
30.0	16.468	9.638	20.496	11.390	24.723	13.341	36.260	19.187	49.416	26.652
40.0	14.513	8.637	17.990	10.155	21.639	11.844	31.597	16.905	42.952	23.364
50.0	12.186	7.473	14.977	8.693	17.905	10.050	25.898	14.115	35.012	19.303
60.0	9.577	6.182	11.594	7.067	13.710	8.051	19.486	10.998	26.073	14.756
70.0	6.627	4.606	7.792	5.098	9.015	5.647	12.353	7.301	16.160	9.424
80.0	3.487	2.698	3.932	2.880	4.400	3.084	5.675	3.701	7.129	4.497

Table B-2. Reflected Solar Spectral Radiance (Continued)

λ = 0.480 μm, $E_{\lambda o}$ = 206.000 mW/cm^2-μm, δ_{TN} = 0.48

ρ	0.00		0.01		0.05		0.10		0.20	
θ_z	L^N	L_A^N	L^N	L_A^N	L^N	L_A^N	L^N	L_A^N	L^N	L_A^N
0.0	5.287	5.287	5.797	5.438	7.854	6.061	10.467	6.881	15.840	8.669
10.0	5.168	5.168	5.668	5.316	7.686	5.927	10.252	6.732	15.526	8.487
20.0	5.036	5.036	5.510	5.177	7.422	5.755	9.850	6.517	14.845	8.179
30.0	4.665	4.665	5.095	4.792	6.833	5.318	9.041	6.012	13.581	7.522
40.0	4.269	4.269	4.641	4.379	6.142	4.833	8.049	5.432	11.971	6.737
50.0	3.900	3.900	4.200	3.988	5.411	4.355	6.950	4.838	10.114	5.890
60.0	3.530	3.530	3.748	3.594	4.628	3.861	5.746	4.212	8.046	4.977
70.0	3.061	3.061	3.192	3.100	3.721	3.260	4.394	3.471	5.776	3.931
80.0	2.144	2.144	2.195	2.159	2.400	2.221	2.660	2.303	3.195	2.481

ρ	0.30		0.40		0.50		0.75		1.00	
θ_z	L^N	L_A^N	L^N	L_A^N	L^N	L_A^N	L^N	L_A^N	L^N	L_A^N
0.0	21.418	10.661	27.213	12.870	33.237	15.309	49.398	22.506	67.336	31.480
10.0	21.001	10.443	26.689	12.611	32.603	15.006	48.466	22.070	66.075	30.880
20.0	20.029	10.030	25.415	12.083	31.015	14.350	46.036	21.039	62.709	29.379
30.0	18.293	9.206	23.189	11.073	28.280	13.134	41.934	19.216	57.090	26.799
40.0	16.043	8.191	20.273	9.803	24.670	11.584	36.467	16.837	49.561	23.387
50.0	13.399	7.063	16.811	8.364	20.359	9.800	26.877	14.037	40.441	19.321
60.0	10.433	5.829	12.913	6.775	15.491	7.818	22.407	10.898	30.084	14.738
70.0	7.211	4.444	8.702	5.012	10.252	5.640	14.410	7.492	19.025	9.801
80.0	3.751	2.679	4.329	2.899	4.929	3.143	6.539	3.860	8.327	4.754

Table B-2. Reflected Solar Spectral Radiance (Continued)

$\lambda = 0.520\ \mu m$, $E_{\lambda o} = 183.400\ mW/cm^2\text{-}\mu m$, $\delta_{TN} = 0.42$

ρ	0.00		0.01		0.05		0.10		0.20	
θ_z	L^N	L_A^N	L^N	L_A^N	L^N	L_A^N	L^N	L_A^N	L^N	L_A^N
0.0	3.565	3.565	4.033	3.690	5.919	4.201	8.310	4.873	13.202	6.329
10.0	3.472	3.472	3.931	3.594	5.783	4.096	8.129	4.755	12.931	6.184
20.0	3.391	3.391	3.827	3.507	5.581	3.983	7.805	4.608	12.356	5.962
30.0	3.118	3.118	3.514	3.223	5.110	3.655	7.132	4.223	11.272	5.454
40.0	2.836	2.836	3.179	2.927	4.562	3.302	6.314	3.795	9.899	4.862
50.0	2.593	2.593	2.870	2.666	3.988	2.969	5.405	3.368	8.306	4.230
60.0	2.365	2.365	2.567	2.418	3.383	2.639	4.416	2.930	6.532	3.559
70.0	2.086	2.086	2.207	2.118	2.698	2.251	3.321	2.425	4.594	2.804
80.0	1.503	1.503	1.549	1.515	1.735	1.566	1.971	1.632	2.454	1.775

ρ	0.30		0.40		0.50		0.75		1.00	
θ_z	L^N	L_A^N	L^N	L_A^N	L^N	L_A^N	L^N	L_A^N	L^N	L_A^N
0.0	18.348	7.940	23.458	9.713	28.837	11.657	43.087	17.317	58.606	24.245
10.0	17.886	7.765	22.999	9.504	28.280	11.411	42.269	16.966	57.502	23.765
20.0	17.051	7.460	21.898	9.110	26.902	10.917	40.160	16.182	54.597	22.626
30.0	15.543	6.816	19.952	8.315	24.504	9.958	36.564	14.745	49.696	20.604
40.0	13.598	6.043	17.416	7.342	21.359	8.767	31.804	12.915	43.178	17.993
50.0	11.298	5.184	14.386	6.235	17.575	7.386	26.024	10.739	35.224	14.845
60.0	8.714	4.256	10.967	5.022	13.293	5.862	19.455	8.309	26.166	11.304
70.0	5.908	3.222	7.265	6.683	8.665	4.188	12.375	5.660	16.415	7.461
80.0	2.952	1.934	3.466	2.108	3.997	2.299	5.403	2.857	6.935	3.540

Table B-2. Reflected Solar Spectral Radiance (Continued)

$\lambda = 0.560\ \mu m$, $E_{\lambda o} = 183.000\ mW/cm^2\text{-}\mu m$, $\delta_{TN} = 0.38$

ρ	0.00		0.01		0.05		0.10		0.20	
θ_z	L^N	L_A^N	L^N	L_A^N	L^N	L_A^N	L^N	L_A^N	L^N	L_A^N
0.0	2.753	2.753	3.223	2.865	5.115	3.324	7.509	3.927	12.392	5.227
10.0	2.670	2.670	3.132	2.780	4.990	3.232	7.341	3.823	12.136	5.101
20.0	2.614	2.614	3.052	2.718	4.813	3.146	7.041	3.707	11.586	4.918
30.0	2.383	2.383	2.781	2.478	4.385	2.867	6.412	3.378	10.549	4.479
40.0	2.153	2.153	2.498	2.235	3.887	2.572	5.643	3.015	9.226	3.939
50.0	1.965	1.965	2.244	2.032	3.369	2.305	4.791	2.663	7.691	3.435
60.0	1.798	1.798	2.002	1.847	2.822	2.046	3.859	2.307	5.973	2.869
70.0	1.599	1.599	1.722	1.629	2.215	1.749	2.839	1.907	4.111	2.247
80.0	1.161	1.161	1.207	1.173	1.390	1.219	1.622	1.280	2.095	1.410

ρ	0.30		0.40		0.50		0.75		1.00	
θ_z	L^N	L_A^N	L^N	L_A^N	L^N	L_A^N	L^N	L_A^N	L^N	L_A^N
0.0	17.405	6.659	22.555	8.226	27.847	9.936	41.736	14.870	56.654	20.832
10.0	17.059	6.506	22.116	8.046	27.312	9.725	40.952	14.571	55.601	20.426
20.0	16.252	6.250	21.045	7.709	25.970	9.300	38.898	13.893	52.782	19.442
30.0	14.796	5.692	19.159	7.020	23.642	8.468	35.409	12.648	48.047	17.698
40.0	12.905	5.019	16.684	6.170	20.567	7.424	30.759	11.045	41.705	14.420
50.0	10.669	4.286	13.729	5.217	16.872	6.233	25.123	9.164	33.984	12.706
60.0	8.144	3.489	10.375	4.167	12.666	4.907	18.682	7.043	25.142	9.924
70.0	5.417	2.621	6.759	3.031	8.137	3.477	11.756	4.766	15.643	6.323
80.0	2.581	1.553	3.080	1.709	3.592	1.879	4.938	2.368	6.383	2.957

Table B-2. Reflected Solar Spectral Radiance (Continued)

λ = 0.620 μm, $E_{\lambda o}$ = 172.400 mW/cm^2-μm, δ_{TN} = 0.33

ρ	0.00		0.01		0.05		0.10		0.20	
θ_z	L^N	L_A^N	L^N	L_A^N	L^N	L_A^N	L^N	L_A^N	L^N	L_A^N
0.0	1.973	1.973	2.428	2.069	4.258	2.464	6.569	2.979	11.266	4.087
10.0	1.905	1.905	2.351	1.999	4.149	2.386	6.417	2.892	11.030	3.978
20.0	1.873	1.873	2.297	1.962	4.001	2.329	6.153	2.809	10.527	3.839
30.0	1.692	1.692	2.078	1.773	3.632	2.108	5.593	2.545	9.581	3.485
40.0	1.520	1.520	1.855	1.591	3.203	1.881	4.905	2.260	8.365	3.074
50.0	1.389	1.389	1.661	1.446	2.757	1.683	4.141	1.992	6.953	2.655
60.0	1.285	1.285	1.485	1.327	2.288	1.500	3.302	1.727	5.364	2.212
70.0	1.166	1.166	1.288	1.192	1.776	1.299	2.393	1.439	3.647	1.739
80.0	0.877	0.877	0.922	0.887	1.102	0.926	1.329	0.977	1.790	1.086

ρ	0.30		0.40		0.50		0.75		1.00	
θ_z	L^N	L_A^N	L^N	L_A^N	L^N	L_A^N	L^N	L_A^N	L^N	L_A^N
0.0	16.067	5.299	20.977	6.619	25.999	8.052	39.070	12.149	52.932	17.036
10.0	15.745	5.168	20.567	6.463	25.498	7.869	38.334	11.890	51.945	16.687
20.0	14.999	4.966	19.572	6.195	24.249	7.528	36.423	11.341	49.332	15.889
30.0	13.657	4.513	17.826	5.634	22.090	6.850	33.186	10.326	44.954	14.474
40.0	11.902	3.965	15.519	4.937	19.218	5.991	28.846	9.005	39.057	12.601
50.0	9.828	3.382	12.769	4.173	15.776	5.031	23.603	7.486	31.903	10.414
60.0	7.471	2.744	9.626	3.324	11.830	3.952	17.567	5.750	23.650	7.895
70.0	4.929	2.067	6.240	2.424	7.581	2.811	11.070	3.916	14.771	5.231
80.0	2.261	1.205	2.744	1.335	3.237	1.476	4.520	1.879	5.881	2.360

Table B-2. Reflected Solar Spectral Radiance (Continued)

$\lambda = 0.660\ \mu m$, $E_{\lambda o} = 156.400\ mW/cm^2\text{-}\mu m$, $\delta_{TN} = 0.29$

ρ	0.00		0.01		0.05		0.10		0.20	
θ_z	L^N	L_A^N	L^N	L_A^N	L^N	L_A^N	L^N	L_A^N	L^N	L_A^N
0.0	1.549	1.549	1.053	1.634	3.725	1.983	5.922	2.438	10.382	3.413
10.0	1.489	1.489	1.916	1.573	3.628	1.916	5.788	2.364	10.171	3.323
20.0	1.471	1.471	1.876	1.550	3.502	1.876	5.553	2.301	9.715	3.211
30.0	1.321	1.321	1.691	1.394	3.177	1.692	5.051	2.080	8.854	2.912
40.0	1.184	1.184	1.506	1.247	2.800	1.506	4.432	1.844	7.745	2.568
50.0	1.088	1.088	1.352	1.140	2.410	1.352	3.745	1.629	6.453	2.222
60.0	1.021	1.021	1.212	1.059	2.000	1.216	2.889	1.421	4.996	1.860
70.0	0.953	0.953	1.074	0.977	1.559	1.074	2.171	1.201	3.413	1.473
80.0	0.768	0.768	0.815	0.777	1.003	0.815	1.241	0.864	1.723	0.969

ρ	0.30		0.40		0.50		0.75		1.00	
θ_z	L^N	L_A^N	L^N	L_A^N	L^N	L_A^N	L^N	L_A^N	L^N	L_A^N
0.0	14.931	4.478	19.571	5.633	24.305	6.883	36.574	10.441	49.499	14.655
10.0	14.642	4.370	19.203	5.507	23.856	6.736	35.914	10.234	48.617	14.377
20.0	13.960	4.204	18.290	5.282	22.708	6.449	34.157	9.768	46.219	13.701
30.0	12.733	3.820	16.689	4.807	20.727	5.873	31.188	8.908	42.210	12.503
40.0	11.123	3.358	14.570	4.216	18.086	5.144	27.198	7.786	36.798	10.915
50.0	9.216	2.869	12.034	3.571	14.910	4.331	22.361	6.493	30.211	9.953
60.0	7.044	2.339	9.132	2.858	11.263	3.421	16.784	5.021	22.600	6.917
70.0	4.680	1.770	5.973	2.092	7.291	2.441	10.708	3.433	14.308	4.607
80.0	2.215	1.083	2.717	1.208	3.229	1.343	4.556	1.726	5.954	2.181

Table B-2. Reflected Solar Spectral Radiance (Continued)

λ = 0.700 μm, $E_{\lambda o}$ = 140.900 mW/cm^2-μm, δ_{TN} = 0.26

ρ	0.00		0.01		0.05		0.10		0.20	
θ_z	L^N	L_A^N	L^N	L_A^N	L^N	L_A^N	L^N	L_A^N	L^N	L_A^N
0.0	1.201	1.201	1.599	1.273	3.202	1.571	5.221	1.959	9.313	2.789
10.0	1.151	1.151	1.543	1.222	3.118	1.515	5.103	1.897	9.125	2.713
20.0	1.140	1.140	1.513	1.208	3.010	1.486	4.896	1.849	8.718	2.625
30.0	1.018	1.018	1.358	1.080	2.728	1.334	4.453	1.666	7.949	2.376
40.0	0.907	0.907	1.205	0.962	2.400	1.184	3.905	1.473	6.957	2.093
50.0	0.836	0.836	1.080	0.880	2.059	1.062	3.293	1.299	5.793	1.805
60.0	0.790	0.790	0.972	0.823	1.702	0.959	2.621	1.136	4.484	1.513
70.0	0.749	0.749	0.862	0.769	1.314	0.851	1.885	0.957	3.040	1.185
80.0	0.623	0.623	0.669	0.632	0.850	0.666	1.079	0.711	1.543	0.807

ρ	0.30		0.40		0.50		0.75		1.00	
θ_z	L^N	L_A^N	L^N	L_A^N	L^N	L_A^N	L^N	L_A^N	L^N	L_A^N
0.0	13.479	3.692	17.719	4.671	22.037	5.726	33.184	8.718	44.864	12.242
10.0	13.220	3.601	17.388	4.563	21.633	5.601	32.590	8.542	44.071	12.007
20.0	12.609	3.469	16.571	4.383	20.604	5.370	31.017	8.166	41.927	11.459
30.0	11.508	3.148	15.130	3.985	18.820	4.888	28.343	7.445	38.322	10.458
40.0	10.063	2.767	13.225	3.497	16.445	4.285	24.757	6.517	33.467	9.146
50.0	8.338	2.357	10.929	2.954	13.568	5.598	20.379	5.425	27.515	7.577
60.0	6.380	1.924	8.311	2.370	10.277	2.850	15.352	4.213	20.670	5.817
70.0	4.216	1.434	5.413	1.704	6.632	1.995	9.779	2.824	13.077	3.803
80.0	2.015	0.912	2.496	1.024	2.986	1.146	4.250	1.490	5.574	1.894

Table B-2. Reflected Solar Spectral Radiance (Continued)

$\lambda = 0.740\ \mu m$, $E_{\lambda o} = 128.300\ mW/cm^2\text{-}\mu m$, $\delta_{TN} = 0.24$

ρ	0.00		0.01		0.05		0.10		0.20	
θ_z	L^N	L_A^N	L^N	L_A^N	L^N	L_A^N	L^N	L_A^N	L^N	L_A^N
0.0	0.956	0.956	1.322	1.019	2.793	1.277	4.645	1.613	8.395	2.331
10.0	0.913	0.913	1.273	0.975	2.719	1.229	4.540	1.560	8.226	2.266
20.0	0.907	0.907	1.249	0.966	2.623	1.207	4.354	1.521	7.857	2.191
30.0	0.804	0.804	1.118	0.858	2.375	1.079	3.958	1.366	7.162	1.979
40.0	0.714	0.714	0.987	0.761	2.086	0.954	3.468	1.205	6.268	1.740
50.0	0.658	0.658	0.882	0.697	1.784	0.855	2.919	1.061	5.217	1.500
60.0	0.625	0.625	0.793	0.654	1.466	0.772	2.314	0.927	4.030	1.255
70.0	0.599	0.599	0.704	0.617	1.126	0.691	1.657	0.788	2.732	0.993
80.0	0.508	0.508	0.550	0.515	0.718	0.545	0.930	0.583	1.358	0.665

ρ	0.30		0.40		0.50		0.75		1.00	
θ_z	L^N	L_A^N	L^N	L_A^N	L^N	L_A^N	L^N	L_A^N	L^N	L_A^N
0.0	12.206	3.110	16.079	3.952	20.018	4.859	30.158	7.419	40.738	10.420
10.0	11.973	3.032	15.781	3.860	19.653	4.752	29.621	7.270	40.023	10.221
20.0	11.417	2.919	15.036	3.705	18.715	4.552	28.188	6.942	38.072	9.745
30.0	10.419	2.644	13.730	3.363	17.096	4.137	25.762	6.324	34.804	8.887
40.0	9.113	2.322	12.005	2.950	14.946	3.627	22.516	5.538	30.416	7.778
50.0	7.552	1.977	9.926	2.493	12.339	3.048	18.553	4.616	25.037	6.454
60.0	5.774	1.612	7.547	1.998	9.349	2.413	13.990	3.585	18.832	4.960
70.0	3.825	1.217	4.936	1.458	6.065	1.718	8.972	2.452	12.006	3.312
80.0	1.793	0.753	2.236	0.849	2.686	0.953	3.844	1.245	5.053	1.587

Table B-2. Reflected Solar Spectral Radiance (Continued)

$\lambda = 0.820\ \mu m$, $E_{\lambda o} = 107.500\ mW/cm^2\text{-}\mu m$, $\delta_{TN} = 0.25$

ρ	0.00		0.01		0.05		0.10		0.20	
θ_z	L^N	L_A^N	L^N	L_A^N	L^N	L_A^N	L^N	L_A^N	L^N	L_A^N
0.0	0.591	0.591	0.878	0.635	2.028	0.816	3.474	1.050	6.396	1.548
10.0	0.562	0.562	0.843	0.605	1.973	0.782	3.393	1.011	6.263	1.500
20.0	0.560	0.560	0.827	0.601	1.899	0.769	3.247	0.986	5.971	1.450
30.0	0.489	0.489	0.733	0.527	1.711	0.680	2.940	0.879	5.426	1.302
40.0	0.428	0.428	0.639	0.460	1.489	0.593	2.558	0.766	4.718	1.134
50.0	0.390	0.390	0.562	0.416	1.254	0.525	2.125	0.665	3.884	0.965
60.0	0.367	0.367	0.494	0.386	1.003	0.466	1.644	0.570	2.938	0.790
70.0	0.345	0.345	0.422	0.357	0.731	0.405	1.120	0.467	1.907	0.601
80.0	0.271	0.271	0.299	0.275	0.410	0.292	0.550	0.315	0.834	0.363

ρ	0.30		0.40		0.50		0.75		1.00	
θ_z	L^N	L_A^N	L^N	L_A^N	L^N	L_A^N	L^N	L_A^N	L^N	L_A^N
0.0	9.359	2.087	12.363	2.668	15.410	3.291	23.219	5.040	31.314	7.075
10.0	9.173	2.028	12.124	2.597	15.116	3.208	22.786	4.923	30.736	6.919
20.0	8.732	1.952	11.533	2.492	14.373	3.072	21.652	4.701	29.197	6.595
30.0	7.945	1.760	10.500	2.253	13.092	2.782	19.733	4.269	26.617	5.998
40.0	6.909	1.532	9.130	1.960	11.382	2.420	17.155	3.712	23.138	5.215
50.0	5.668	1.290	7.477	1.639	9.311	2.014	14.013	3.067	18.886	4.291
60.0	4.251	1.028	5.582	1.285	6.931	1.561	10.390	2.335	13.976	3.235
70.0	2.704	0.745	3.513	0.901	4.333	1.068	6.434	1.537	8.613	2.082
80.0	1.121	0.415	1.412	0.471	1.707	0.531	2.464	0.699	3.249	0.895

Table B-2. Reflected Solar Spectral Radiance (Continued)

λ = 0.880 μm, $E_{\lambda o}$ = 96.300 mW/cm^2-μm, δ_{TN} = 0.19

ρ	0.00		0.01		0.05		0.10		0.20	
θ_z	L^N	L_A^N	L^N	L_A^N	L^N	L_A^N	L^N	L_A^N	L^N	L_A^N
0.0	0.524	0.524	0.810	0.565	1.959	0.733	3.403	0.951	6.319	1.416
10.0	0.497	0.497	0.778	0.537	1.908	0.703	3.328	0.917	6.196	1.375
20.0	0.497	0.497	0.765	0.536	1.841	0.693	3.192	0.898	5.922	1.334
30.0	0.435	0.435	0.680	0.470	1.666	0.614	2.905	0.801	5.407	1.200
40.0	0.382	0.382	0.597	0.413	1.461	0.539	2.548	0.703	4.742	1.053
50.0	0.352	0.352	0.530	0.378	1.244	0.483	2.142	0.618	3.954	0.908
60.0	0.341	0.341	0.475	0.360	1.014	0.439	1.691	0.541	3.058	0.759
70.0	0.338	0.338	0.424	0.350	0.769	0.401	1.203	0.466	2.078	0.605
80.0	0.310	0.310	0.346	0.315	0.492	0.337	0.674	0.364	1.042	0.423

ρ	0.30		0.40		0.50		0.75		1.00	
θ_z	L^N	L_A^N	L^N	L_A^N	L^N	L_A^N	L^N	L_A^N	L^N	L_A^N
0.0	9.273	1.919	12.265	2.460	15.298	3.041	23.056	4.671	31.078	6.565
10.0	9.102	1.869	12.045	2.402	15.027	2.973	22.658	4.577	30.549	6.441
20.0	8.688	1.805	11.489	2.313	14.328	2.857	21.591	4.385	29.102	6.160
30.0	7.942	1.631	10.510	2.095	13.111	2.593	19.768	3.991	26.652	5.616
40.0	6.964	1.431	9.216	1.838	11.497	2.275	17.334	3.502	23.371	4.927
50.0	5.790	1.220	7.650	1.557	9.535	1.918	14.357	2.932	19.344	4.110
60.0	4.444	0.994	5.847	1.247	7.269	1.520	10.907	2.283	14.669	3.171
70.0	2.966	0.756	3.864	0.918	4.775	1.092	7.105	1.581	9.514	2.149
80.0	1.416	0.487	1.794	0.555	2.177	0.628	3.157	0.835	4.171	1.074

Table B-2. Reflected Solar Spectral Radiance (Continued)

λ = 1.050 μm, $E_{\lambda o}$ = 63.300 mW/cm^2-μm, δ_{TN} = 0.15

ρ	0.00		0.01		0.05		0.10		0.20	
θ_z	L^N	L^N_A	L^N	L^N_A	L^N	L^N_A	L^N	L^N_A	L^N	L^N_A
0.0	0.263	0.263	0.465	0.287	1.273	0.386	2.289	0.514	4.336	0.786
10.0	0.247	0.247	0.446	0.271	1.241	0.368	2.240	0.494	4.254	0.762
20.0	0.249	0.249	0.438	0.272	1.196	0.365	2.148	0.485	4.066	0.740
30.0	0.214	0.214	0.388	0.235	1.083	0.320	1.957	0.430	3.718	0.664
40.0	0.186	0.186	0.338	0.204	0.949	0.279	1.717	0.375	3.264	0.581
50.0	0.172	0.172	0.298	0.187	0.805	0.249	1.441	0.329	2.724	0.499
60.0	0.168	0.168	0.264	0.180	0.649	0.227	1.133	0.288	2.109	0.417
70.0	0.171	0.171	0.234	0.179	0.484	0.209	0.799	0.249	1.432	0.333
80.0	0.166	0.166	0.194	0.170	0.303	0.183	0.440	0.200	0.716	0.237

ρ	0.30		0.40		0.50		0.75		1.00	
θ_z	L^N	L^N_A	L^N	L^N_A	L^N	L^N_A	L^N	L^N_A	L^N	L^N_A
0.0	6.404	1.080	8.494	1.395	10.606	1.732	15.984	2.673	21.507	3.759
10.0	6.288	1.050	8.344	1.360	10.422	1.692	15.712	2.617	21.146	3.686
20.0	6.003	1.015	7.962	1.311	9.940	1.627	14.980	2.509	20.155	3.528
30.0	5.497	0.917	7.295	1.188	9.111	1.478	13.738	2.287	18.489	3.222
40.0	4.828	0.803	6.407	1.041	8.004	1.295	12.069	2.006	16.244	2.827
50.0	4.020	0.683	5.330	0.880	6.654	1.091	10.025	1.681	13.486	2.361
60.0	3.094	0.557	4.090	0.708	5.097	0.868	7.659	1.317	10.291	1.835
70.0	2.073	0.424	2.720	0.522	3.374	0.626	5.039	0.918	6.749	1.255
80.0	0.995	0.277	1.277	0.320	1.562	0.366	2.288	0.494	3.034	0.641

Table B-2. Reflected Solar Spectral Radiance (Continued)

λ = 1.250 μm, $E_{\lambda o}$ = 46.400 mW/cm^2-μm, δ_{TN} = 0.13

ρ	0.00		0.01		0.05		0.10		0.20	
θ_z	L^N	L_A^N	L^N	L_A^N	L^N	L_A^N	L^N	L_A^N	L^N	L_A^N
0.0	0.139	0.139	0.279	0.153	0.840	0.211	1.544	0.285	2.961	0.614
10.0	0.130	0.130	0.267	0.144	0.820	0.200	1.512	0.274	2.907	0.430
20.0	0.132	0.132	0.263	0.145	0.788	0.199	1.448	0.269	2.776	0.417
30.0	0.112	0.112	0.232	0.124	0.715	0.173	1.320	0.237	2.539	0.374
40.0	0.095	0.095	0.201	0.106	0.625	0.149	1.157	0.206	2.228	0.325
50.0	0.087	0.087	0.175	0.096	0.527	0.132	0.968	0.179	1.856	0.278
60.0	0.086	0.086	0.153	0.093	0.420	0.120	0.755	0.156	1.430	0.231
70.0	0.088	0.088	0.132	0.093	0.305	0.111	0.523	0.134	0.961	0.183
80.0	0.087	0.087	0.106	0.089	0.181	0.096	0.275	0.106	0.465	0.127

ρ ρ	0.30		0.40		0.50		0.75		1.00	
θ_z	L^N	L_A^N	L^N	L_A^N	L^N	L_A^N	L^N	L_A^N	L^N	L_A^N
0.0	4.390	0.614	5.832	0.796	7.286	0.991	10.975	1.534	14.746	2.157
10.0	4.313	0.597	5.731	0.777	7.162	0.969	10.793	1.504	14.503	2.118
20.0	4.115	0.576	5.465	0.747	6.827	0.930	10.284	1.438	13.816	2.022
30.0	3.769	0.520	5.008	0.677	6.259	0.845	9.433	1.312	12.676	1.849
40.0	3.307	0.453	4.396	0.591	5.495	0.738	8.283	1.148	11.131	1.618
50.0	2.751	0.385	3.654	0.499	4.565	0.621	6.876	0.961	9.238	1.315
60.0	2.110	0.312	2.796	0.399	3.489	0.491	5.245	0.750	7.041	1.046
70.0	1.404	0.236	1.849	0.292	2.299	0.352	3.440	0.520	4.607	0.713
80.0	0.656	0.150	0.849	0.174	1.044	0.200	1.538	0.273	2.043	0.356

Table B-2. Reflected Solar Spectral Radiance (Continued)

$\lambda = 1.600\ \mu m$, $E_{\lambda o} = 24.900\ mW/cm^2\text{-}\mu m$, $\delta_{TN} = 0.10$

ρ	0.00		0.01		0.05		0.10		0.20	
θ_z	L^N	L_A^N	L^N	L_A^N	L^N	L_A^N	L^N	L_A^N	L^N	L_A^N
0.0	0.054	0.054	0.130	0.060	0.436	0.084	0.820	0.116	1.591	0.184
10.0	0.050	0.050	0.125	0.056	0.426	0.080	0.804	0.111	1.563	0.178
20.0	0.051	0.051	0.122	0.056	0.409	0.080	0.769	0.110	1.492	0.173
30.0	0.042	0.042	0.108	0.048	0.372	0.069	0.702	0.096	1.367	0.155
40.0	0.036	0.036	0.094	0.040	0.326	0.059	0.617	0.083	1.201	0.134
50.0	0.033	0.033	0.081	0.036	0.274	0.052	0.516	0.072	1.002	0.115
60.0	0.032	0.032	0.069	0.035	0.217	0.047	0.402	0.063	0.773	0.095
70.0	0.034	0.034	0.058	0.036	0.155	0.044	0.277	0.054	0.521	0.075
80.0	0.035	0.035	0.046	0.036	0.089	0.039	0.144	0.044	0.253	0.054

ρ	0.30		0.40		0.50		0.75		1.00	
θ_z	L^N	L_A^N	L^N	L_A^N	L^N	L_A^N	L^N	L_A^N	L^N	L_A^N
0.0	2.367	0.257	3.149	0.335	3.936	0.418	5.925	0.649	7.948	0.913
10.0	2.327	0.250	3.095	0.326	3.870	0.408	5.827	0.635	7.818	0.895
20.0	2.220	0.241	2.953	0.314	3.690	0.392	5.555	0.609	7.452	0.857
30.0	2.036	0.217	2.709	0.285	3.387	0.356	5.101	0.555	6.844	0.783
40.0	1.790	0.190	2.382	0.249	2.979	0.312	4.487	0.487	6.021	0.687
50.0	1.492	0.161	1.984	0.210	2.480	0.262	3.735	0.408	5.011	0.575
60.0	1.148	0.130	1.524	0.168	1.903	0.208	2.862	0.320	3.837	0.447
70.0	0.767	0.098	1.014	0.123	1.263	0.149	1.894	0.223	2.534	0.306
80.0	0.363	0.064	0.474	0.075	0.586	0.087	0.869	0.120	1.156	0.158

Table B-2. Reflected Solar Spectral Radiance (Continued)

λ = 2.200 μm, $E_{\lambda o}$ = 8.300 mW/cm^2-μm, δ_{TN} = 0.13

ρ	0.00		0.01		0.05		0.10		0.20	
θ_z	L^N	L_A^N	L^N	L_A^N	L^N	L_A^N	L^N	L_A^N	L^N	L_A^N
0.0	0.011	0.011	0.034	0.013	0.126	0.018	0.241	0.025	0.471	0.040
10.0	0.010	0.010	0.033	0.012	0.123	0.017	0.236	0.024	0.462	0.039
20.0	0.011	0.011	0.032	0.012	0.118	0.017	0.225	0.024	0.440	0.038
30.0	0.009	0.009	0.028	0.010	0.107	0.015	0.205	0.021	0.402	0.033
40.0	0.007	0.007	0.024	0.008	0.093	0.013	0.179	0.018	0.351	0.029
50.0	0.007	0.007	0.021	0.007	0.077	0.011	0.147	0.015	0.289	0.024
60.0	0.006	0.006	0.017	0.007	0.059	0.009	0.112	0.013	0.218	0.019
70.0	0.006	0.006	0.013	0.007	0.040	0.008	0.073	0.010	0.140	0.015
80.0	0.006	0.006	0.008	0.006	0.019	0.007	0.032	0.007	0.058	0.009

ρ	0.30		0.40		0.50		0.75		1.00	
θ_z	L^N	L_A^N	L^N	L_A^N	L^N	L_A^N	L^N	L_A^N	L^N	L_A^N
0.0	0.702	0.056	0.935	0.073	1.169	0.092	1.758	0.142	2.355	0.200
10.0	0.690	0.054	0.919	0.071	1.149	0.089	1.728	0.139	2.315	0.196
20.0	0.657	0.053	0.874	0.069	1.093	0.086	1.644	0.133	2.202	0.188
30.0	0.600	0.047	0.799	0.062	0.999	0.077	1.503	0.120	2.013	0.170
40.0	0.524	0.041	0.698	0.054	0.873	0.067	1.313	0.105	1.759	0.149
50.0	0.431	0.034	0.574	0.045	0.718	0.056	1.080	0.087	1.447	0.123
60.0	0.324	0.027	0.431	0.035	0.539	0.043	0.810	0.066	1.084	0.093
70.0	0.207	0.019	0.274	0.024	0.342	0.029	0.513	0.044	0.686	0.061
80.0	0.085	0.011	0.111	0.013	0.138	0.015	0.205	0.021	0.273	0.027

APPENDIX C

SENSOR FIELD OF VIEW

Each time the satellite completes an orbit around the Earth, it maps out a swath on the Earth's surface of width S_w. The angle subtended at the satellite by S_W is the sensor field of view Θ. Referring to Figure 1 and using the law of cosines, one can write

$$\Theta = 2 \text{ Cos}^{-1} \left(\frac{R^2{}_S + S^2{}_d - R^2{}_e}{2S_d R_S} \right) \quad [\text{rad}] \ , \tag{C-1}$$

where

$$R_S = H + R_e \quad [\text{km}] \tag{C-2}$$

and

$$S_d = \left[R_S^2 + R_e^2 - 2R_S R_e \text{ Cos} \left(\frac{\Phi_S}{2} \right) \right]^{1/2} \quad [\text{km}] \ . \tag{C-3}$$

From Figure 1, it can also be seen that

$$\Phi_S = \frac{S_W}{R_e} \quad [\text{rad}] \ . \tag{C-4}$$

The swath width S_W is given by

$$S_W = \frac{Ad_C}{N_S} \quad [\text{km}] \tag{C-5}$$

where d_C is the cross-track distance covered by the sensor and, for total coverage at the equator, is given by

$$d_C = 2\pi R_e \quad [\text{km}] \ . \tag{C-6}$$

Now, if the total time required to map the Earth t_{MAP} is known, then the total number of swaths N_S required to map the Earth is

$$N_S = \frac{t_{MAP}}{t_S} \quad [\text{nd}] \ , \tag{C-7}$$

where t_S is the satellite's orbital period or the time required to map one swath and is given by

$$t_S = \frac{2\pi R_e}{V_{SUB}} \quad [\text{sec}] \ . \tag{C-8}$$

Finally, the cross-track overlap factor A is given by,

$$A = \left(1 + \frac{S'_o}{100} \right) \quad [\text{nd}] \ , \tag{C-9}$$

where S'_o is the percentage overlap across the ground track.

APPENDIX D

VIEW FACTOR FOR A SINGLE DETECTOR VIEWING A CIRCULAR BACKGROUND

The view factor F_C for a detector that is receiving radiation from a circular background can be defined as

$$F_C = \frac{\Phi'}{\pi A_D L'_{\Delta\lambda}} \quad [\text{nd}] \ , \tag{D-1}$$

where Φ' = the photon flux into the detector [p/sec],

A_D = the area of the detector [cm^2],

and

$$L'_{\Delta\lambda} = \int_0^{\lambda_c} B'(\lambda, T_{BG})\ d\lambda \qquad [\text{p/sec-cm}^2\text{-sr}] \ , \tag{D-2}$$

where $B'(\lambda, T_{BG})$ = Planck's function evaluated at the background temperature T_{BG}, and

λ_c = the detector cutoff wavelength.

If a detector of area A_D views a source of radiance $L'_{\Delta\lambda}$ with area dA' through a solid angle Ω, the flux into the detector is

$$d\Phi' = L'_{\Delta\lambda}\Omega\ \text{Cos}(\phi'_c)\ dA' \qquad [\text{p/sec}] \ . \tag{D-3}$$

The angle ϕ'_c is shown in Figure D-1.

However,

$$dA' = 2\pi r'\ dr' \qquad [\text{cm}^2] \tag{D-4}$$

and

$$\Omega = \frac{A_D\ \text{Cos}(\phi'_c)}{S^2} \qquad [\text{sr}] \ . \tag{D-5}$$

Substituting Equations (D-4) and (D-5) into Equation (D-3) gives

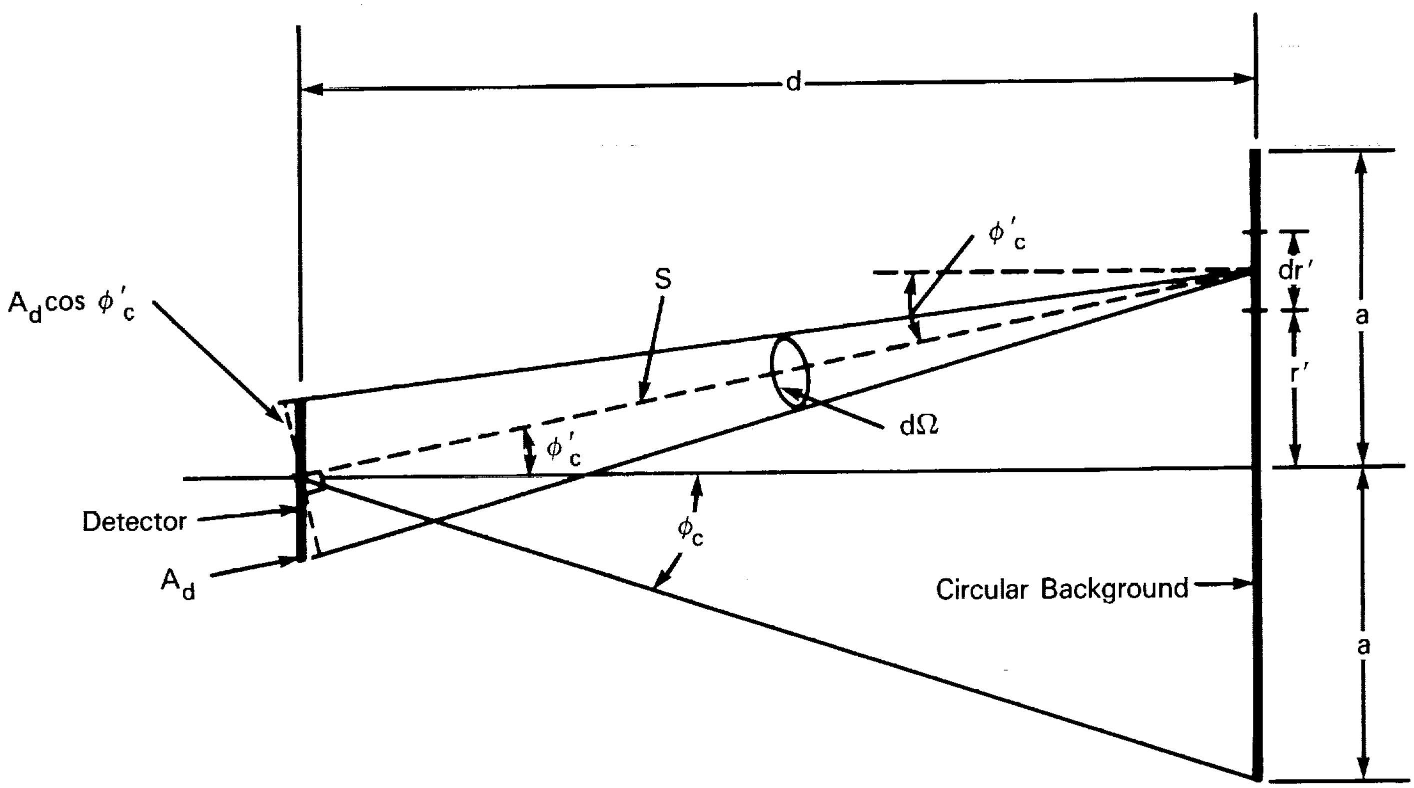

a = Circular background radius (cm)
A_d = Area of detector (μm)
d = Distance between the detector and the circular background (cm)
dA' = $2\pi r'dr'$ = Area of elemental annular ring of radius r' (cm^2)
S = Distance from center of detector to elemental area on circular background (cm)
ϕ_c = Half angle subtended by the circular background at the center of the detector (deg)
ϕ'_c = Half angle subtended by the elemental circular area dA' at the center of the detector (deg)
$d\Omega$ = Elemental solid angle subtended by the detector at a point on the elemental area dA' (sr)

Figure D-1. View Factor Geometry for a Single Detector Viewing a Circular Background

$$d\Phi' = \frac{2\pi r A_D L'_{\Delta\lambda} \, \mathrm{Cos}^2(\phi'_c) dr'}{S^2} \quad [\mathrm{p/sec}] \; . \tag{D-6}$$

However, from Figure D-1 we see that

$$\mathrm{Cos}\; \phi'_c = \frac{d}{S} = \frac{d}{\left(d^2 + r'^2\right)^{1/2}} \quad [\mathrm{rad}] \; , \tag{D-7}$$

and substituting Equation (D-7) into Equation (D-6) gives

$$d\Phi' = 2\pi d^2 \; A_D L'_{\Delta\lambda} \; \frac{r' \; dr'}{\left(d^2 + r'^2\right)^2} \quad [\mathrm{p/sec}] \; . \tag{D-8}$$

It follows that

$$\Phi' = 2\pi d^2 \; A_D L'_{\Delta\lambda} \int_0^a \frac{r' \; dr'}{\left(d^2 + r'^2\right)^2} \quad [\mathrm{p/sec}] \; . \tag{D-9}$$

However,

$$\int_0^a \frac{r' \; dr'}{\left(d^2 + r'^2\right)^2} = \frac{1}{2\; d^2} - \frac{1}{2\left(d^2 + a^2\right)} \; . \tag{D-10}$$

Therefore, substituting Equation (D-10) into Equation (D-9) gives

$$\Phi' = \pi A_D L'_{\Delta\lambda} \left(1 - \frac{d^2}{d^2 + a^2}\right) \; [\mathrm{p/sec}] \; . \tag{D-11}$$

However,

$$\frac{d}{\left(d^2 + a^2\right)^{1/2}} = \frac{d}{S_a} = \mathrm{Cos}\; \phi_c \quad [\mathrm{nd}] \; . \tag{D-12}$$

Therefore, by substituting Equation (D-12) into Equation (D-11) we obtain

$$\Phi' = \pi A_D L'_{\Delta\lambda} \; \mathrm{Sin}^2 \; \phi_c \quad [\mathrm{p/sec}] \; . \tag{D-13}$$

APPENDIX E

VIEW FACTOR FOR A DETECTOR IN AN n X m ARRAY VIEWING A RECTANGULAR BACKGROUND

The view factor F_A for a detector in an n by m array viewing a rectangular background (Figure E-1) is given by

$$F_A = \frac{\Phi'}{\pi A_D L'_{\Delta\lambda}} \qquad \text{(E-1)}$$

where Φ' is the total number of photons per second entering the detector from the background through a rectangular aperture, given by

$$\Phi' = L'_{\Delta\lambda} \int_0^{A_b} \Omega_d \operatorname{Cos} \phi_f \, dA_B \qquad [\text{p/sec}] \qquad \text{(E-2)}$$

and, as in Appendix D, $L'_{\Delta\lambda}$ is

$$L'_{\Delta\lambda} = \int_0^{\lambda_c} B'(\lambda, T_{BG}) d\lambda \qquad [\text{p/sec–cm}^2\text{–sr}]$$

where the photon radiance $L'_{\Delta\lambda}$ is given by Equation (E-2) and

where $B'(\lambda,T_{BG})$ = the Planck function evaluated at the background temperature T_{BG} [p/sec–cm^2–sr–μm];

Ω_D = the solid angle subtended by the detector at an arbitrary point on the rectangular aperture through which the background is viewed;

dA_B = the differential area on the background; and

ϕ_f = the angle between the normal to the differential area dA_B and the line between the center of the detector and the center of the differential area dA_B.

If D is the distance between the center of the detector and the differential area dA_B then

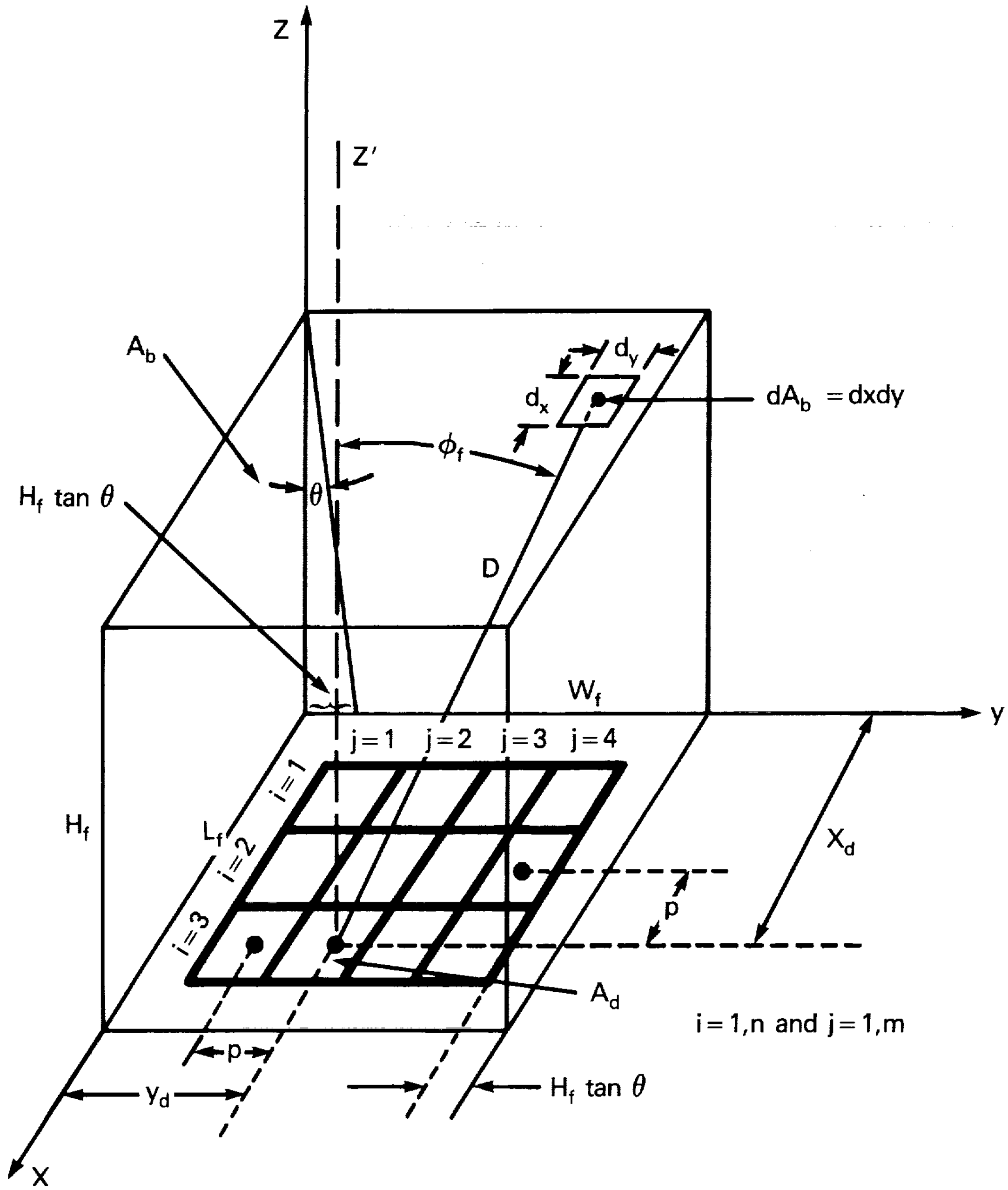

A_b = Background area (cm^2)
A_d = Detector area (μm^2)
D = Distance from center of detector to dA_b (cm)
dA_b = Differental background area (cm^2)
H_f = Fence height (cm)
L_f = Fence length (cm)
p = Detector pitch (cm)
W_f = Fence width (cm)
θ = Optics half-cone angle (deg)
ϕ_f = Differential area normal angle

Figure E-1. Geometry for a Detector in n X m Array Viewing a Rectangular Background

$$\Omega_d = \frac{A_d \; \mathrm{Cos}(\phi_f)}{D^2} \qquad [\mathrm{sr}] \ , \tag{E-3}$$

where

$$\mathrm{Cos}(\phi_f) = \frac{z}{D} \qquad [\mathrm{nd}] \ . \tag{E-4}$$

To evaluate the quantities D, ϕ_f, and z in Equations E-3 and E-4, it is convenient to define two sets of coordinates. The two systems (x,y,z) and (x′,y′,z′) are shown in Figure E-1. The n X m detector array lies in the x-y plane and the plane of the rectangular aperture, through which the background is viewed, is a distance H_f from the x-y plane.

Consider an n X m array of detectors, and let p be the pitch (distance between detector centers) in both directions (Figure E-1). Let the detector array be symmetrically surrounded by very cold sides (fence) of length L_f, width W_f, and height H_f. The length and width are adjusted for a given height so that the edge detectors in the array can just accommodate the optical bundle which is defined by half the bundle cone angle θ. The relationships for the length L_f and width W_f of the fenced area that surrounds the detector array are

$$L_f = np + 2H_f \; \mathrm{Tan}(\theta) \qquad [\mathrm{m}] \ , \tag{E-5}$$

and

$$W_f = mp + 2H_f \; \mathrm{Tan}(\theta) \qquad [\mathrm{m}] \ , \tag{E-6}$$

where n = the number of detectors along the length of the detector array, and

m = the number of detectors along the width of the detector array.

Equations (E-5) and (E-6) follow because

$$\mathrm{Sin}(\theta) = \frac{1}{2f_n} \ . \tag{E-7}$$

The coordinates of detector i, j with respect to the edges of the fenced area are given by

$$x_d = H_f \, \mathrm{Tan}(\theta) - \frac{p}{2} + ip \tag{E-8}$$

and

$$y_d = H_f \, \mathrm{Tan}(\theta) - \frac{p}{2} + jp \ , \tag{E-9}$$

where i = the number of detectors along the fence length, (i = 1, ..., n) and

j = the number of detectors along the fence width, (j = 1, ..., m).

The coordinates of the arbitrarily placed differential area dA_B on the surface formed by the top edges of the fence are (x,y,z). The coordinates with respect to the center of the detector i, j are given by

$$x' = x - x_d \ , \tag{E-10}$$

$$y' = y - y_d \ , \tag{E-11}$$

and

$$z' = z \ , \tag{E-12}$$

where

$$z = H_f \tag{E-13}$$

and

$$D = \left(x'^2 + y'^2 + z'^2 \right)^{1/2} \ . \tag{E-14}$$

By substituting Equations (E-10) through (E-13) into Equation (E-14), one gets

$$D = \left[\left(x - x_d \right)^2 + \left(y - y_d \right)^2 + z^2 \right]^{1/2} \ . \tag{E-15}$$

Letting

$$dA_b = dx \ dy \tag{E-16}$$

and substituting Equations (E-3), (E-4), (E-13), and (E-16) into Equation (E-2) results in

$$\Phi' = A_D \ H_f^2 \ B'_{\Delta\lambda} \int_0^{W_f} \int_0^{L_f} \frac{dx \ dy}{D^4} \quad [\text{p/sec}] \ . \tag{E-17}$$

Substituting Equation (E-17) into Equation (E-1) yields

$$F_A = \frac{H_f^2}{\pi} \int_0^{W_f} g(y)\, dy \, , \tag{E-18}$$

where

$$g(y) = \int_0^{L_f} \frac{dx}{D^4} \, . \tag{E-19}$$

Equation (E-19) may also be written as

$$g(y) = \int_0^{L_f} \frac{dx}{X^2} \, , \tag{E-20}$$

where

$$X = ax^2 + bx + c \tag{E-21}$$

$$a = 1 \tag{E-22}$$

$$b = -2x_d \tag{E-23}$$

and

$$c = x_d^2 + (y - y_d)^2 + z^2 \, . \tag{E-24}$$

It follows from Equations (E-22) through (E-24) that

$$4ac - b^2 = 4(y - y_d)^2 + 4z^2 \, . \tag{E-25}$$

Now, Equation (E-25) reveals that

$$4ac > b^2 \, . \tag{E-26}$$

Therefore, Equation (E-20) may be written (Dwight, 1947, p. 33, Equations 160.01 and 160.02) as

$$\int \frac{dx}{X^2} = \frac{2ax + b}{rX} + \frac{4a}{R_2} \; \mathrm{Tan}^{-1} \left(\frac{2ax + b}{R_1} \right) , \tag{E-27}$$

where

$$r = 4ac - b^2 \tag{E-28}$$

and

$$R_1 = r^{1/2} = \left(4ac - b^2 \right)^{1/2} \tag{E-29}$$

and

$$R_2 = rR_1 = r^{3/2} . \tag{E-30}$$

Applying Equation (E-27) to Equation (E-28), one gets

$$g(y) = \frac{2aL_f + b}{r\left(aL_f^2 + bL_f + c \right)} + \frac{4a}{R_2} \; \mathrm{Tan}^{-1} \left(\frac{2aL_f + b}{R_1} \right)$$

$$- \frac{b}{r\,c} - \frac{4a}{R_2} \; \mathrm{Tan}^{-1} \left(\frac{b}{R_1} \right) \tag{E-31}$$

Use of Equation (E-31) in Equation (E-18) and numerical integration enable the form factor F_A to be computed.

APPENDIX F

COMPUTATION OF γ

Substituting Equations (2-11) and (2-12) into Equation (2-9) yields

$$S' = t_I \tau_o A_D \eta \left(\frac{\lambda}{hc}\right) \left(\frac{\pi}{4f^2_N}\right) \int_{\lambda_1}^{\lambda_2} L(\lambda)\, d\lambda \quad [e] \ . \tag{F-1}$$

Therefore, the signal equation for the visible and SWIR bands is given by

$$S' = t_I \tau_o A_D \eta \left(\frac{\lambda}{hc}\right) \left(\frac{\pi}{4f^2_N}\right) L\Delta\lambda \quad [e] \tag{F-2}$$

where we have replaced the integral in Equation (F-1) by $L\Delta\lambda$ because $L(\lambda)$ varies slowly over the spectral bandpass $\Delta\lambda$. Taking the differential of Equation (F-2) with respect to the scene radiance, one obtains

$$dS' = t_I \tau_o A_D \eta \left(\frac{\lambda}{hc}\right) \left(\frac{\pi}{4f^2_N}\right) dL\ \Delta\lambda \quad [e] \ . \tag{F-3}$$

Dividing Equation (F-2) by (F-3) gives

$$\frac{S}{N} = \frac{S'}{dS'} = \frac{L}{dL} \quad [nd] \tag{F-4}$$

where the signal $S = S'$, and the noise $N = dS'$.

However,

$$dL = \left(\frac{dL}{d\rho}\right) d\rho \qquad [W/cm^2\text{-}sr\text{-}\mu m] \ . \tag{F-5}$$

Substituting Equation (F-5) into Equation (F-4) gives

$$\frac{S}{N} = \frac{L}{\left(\frac{dL}{d\rho}\right) d\rho} \quad [nd] \ . \tag{F-6}$$

Letting

$$\gamma \equiv \frac{L}{\left(\frac{dL}{d\rho}\right)} \quad [\text{nd}] \ , \tag{F-7}$$

$$d\rho \equiv NE\Delta\rho \tag{F-8}$$

and substituting Equations (F-7) and (F-8) into Equation (F-5), one obtains

$$\frac{S}{N} = \frac{\gamma}{NE\Delta\rho} \ . \tag{F-9}$$

However,

$$L = L_S^S + L_A^S \quad [\text{W/cm}^2\text{-sr-}\mu\text{m}] \tag{F-10}$$

where the surface spectral radiance L_S^S has the functional form

$$L_S^S = \rho K_1 \quad [\text{W/cm}^2\text{-sr-}\mu\text{m}] \tag{F-11}$$

and the atmospheric spectral radiance is a constant with respect to ρ and is given by

$$L_A^S = K_2 \quad [\text{W/cm}^2\text{-sr-}\mu\text{m}] \tag{F-12}$$

The superscript S denotes that the sensor observes these spectral radiances along a slanted path. (See Figure 6.) Since the scene spectral radiances are assumed to be equal in the normal and slant directions, no superscript is used.

Substituting Equations (F-11) and (F-12) into Equation (F-10) gives

$$L = K_1\rho + K_2 \quad [\text{W/cm}^2\text{-sr-}\mu\text{m}] \ . \tag{F-13}$$

Differentiating Equation (F-13) with respect to ρ results in

$$\frac{dL}{d\rho} = K_1 \quad [\text{W/cm}^2\text{-sr-}\mu\text{m}] \tag{F-14}$$

Solving for K_1 in Equation (F-11) and substituting it into Equation (F-14) results in

$$\frac{dL}{d\rho} = \frac{L_S^S}{\rho} \quad [\text{W/cm}^2\text{-sr-}\mu\text{m}] \ . \tag{F-15}$$

Substituting Equation (F-15) into Equation (F-7) gives

$$\gamma = \left(\frac{L}{L_S^S}\right)\rho \quad [\mathrm{nd}] \ . \tag{F-16}$$

The spectral radiances L and L_S^S are observed along the line-of-sight direction with angle of ϕ and a line-of-sight surface-normal angle ϕ' (Figure 6). These angles are related by

$$\phi' = \mathrm{Sin}^{-1}\left[\left(1 + \frac{H}{R_e}\right)\sin\phi\right] \quad [\mathrm{rad}] \ . \tag{F-17}$$

The surface spectral radiance L_S^S is given by

$$L_S^S = \frac{E_S}{\pi}\,\rho\tau_{AN}^{\mathrm{Sec}(\phi')} \quad [\mathrm{W/cm^2\text{-}sr\text{-}\mu m}] \tag{F-18}$$

where E_S = the irradiance at the surface of the Earth $[\mathrm{W/cm^2\text{-}\mu m}]$

The atmospheric transmission along the nadir direction is given by

$$\tau_{AN} = e^{-\delta_o} \quad [\mathrm{nd}] \ , \tag{F-19}$$

where δ_o is the optical depth along the nadir direction. (See Appendix B)

The surface spectral radiance L_S observed along the nadir direction (for which $\phi' = 0$) is given by

$$L_S^N = \frac{E_S}{\pi}\,\rho\tau_{AN} \quad [\mathrm{W/cm^2\text{-}sr\text{-}\mu m}] \ . \tag{F-20}$$

Dividing Equation (F-18) by Equation (F-19) gives

$$L_S^S = L_S^N\,\tau_{AN}^{(\mathrm{Sec}\,\phi' - 1)} \quad [\mathrm{W/cm^2\text{-}sr\text{-}\mu m}] \ . \tag{F-21}$$

Substituting Equation (F-21) into Equation (F-16) we obtain

$$\gamma = \frac{\gamma_o}{\tau_{AN}^{(\mathrm{Sec}\,\phi' - 1)}} \quad [\mathrm{nd}] \tag{F-22}$$

where

$$\gamma_o = \frac{L\rho}{L_S^N} \qquad [nd] \ . \tag{F-23}$$

We assume the total spectral radiance L is the same along the nadir and slant directions; hence

$$L = L_S^N + L_A^N \qquad [W/cm^2\text{-sr-}\mu m] \tag{F-24}$$

or

$$L_S^N = L - L_A^N \qquad [W/cm^2\text{-sr-}\mu m] \ . \tag{F-25}$$

Substituting Equation (F-25) into Equation (F-23) gives

$$\gamma_o = \left[\frac{L}{L - L_A^N}\right]\rho \qquad [nd] \tag{F-26}$$

or

$$\gamma_o = \frac{\rho}{\left[1 - \frac{L_A^N}{L}\right]} \qquad [nd] \ . \tag{F-27}$$

APPENDIX G

NOISE EQUIVALENT DELTA TEMPERATURE

Equation (2-9) enables the signal to be written as

$$S' = t_I A_D \eta E'_{\Delta\lambda} \quad [e] \ , \tag{G-1}$$

where

$$E'_{\Delta\lambda} = \int_{\lambda_1}^{\lambda_2} E'(\lambda)\ d\lambda \qquad [p/sec\text{-}cm^2] \ . \tag{G-2}$$

However,

$$E'(\lambda) = \frac{\pi\tau_o}{4f^2_N}\ L'(\lambda) \qquad [p/sec\text{-}cm^2\text{-}\mu m] \tag{G-3}$$

and

$$L'(\lambda) = \tau_A B'(\lambda,T_S) + \epsilon_A B'(\lambda,T_A) \qquad [p/sec\text{-}cm^2\text{-}sr\text{-}\mu m] \ . \tag{G-4}$$

Therefore,

$$E'_{\Delta\lambda} = \frac{\pi\tau_o}{4f^2_N}\ L'_{\Delta\lambda} \qquad [p/sec\text{-}cm^2] \tag{G-5}$$

where

$$L'_{\Delta\lambda} = \int_{\lambda_1}^{\lambda_2} L'(\lambda)\ d\lambda \qquad [p/sec\text{-}cm^2\text{-}sr] \ . \tag{G-6}$$

Equation (G-4) can be written as

$$L'_{\Delta\lambda} = \tau_A L'_{S\Delta\lambda} + \epsilon_A L'_{A\Delta\lambda} \qquad [p/sec\text{-}cm^2\text{-}sr] \ , \tag{G-7}$$

where

$$L'_{S\Delta\lambda} = \int_{\lambda_1}^{\lambda_2} B'(\lambda,T_S)\ d\lambda \qquad [p/sec\text{-}cm^2\text{-}sr] \tag{G-8}$$

and

$$L'_{A\Delta\lambda} = \int_{\lambda_1}^{\lambda_2} B'(\lambda,T_A)\, d\lambda \qquad [p/sec\text{-}cm^2\text{-}sr] \; . \tag{G-9}$$

Taking the differential of Equation (G-1), one obtains

$$dS' = (t_I A_D \eta)\, dE'_{\Delta\lambda} \qquad [e] \; . \tag{G-10}$$

Replacing dS' by N, and $dE'_{\Delta\lambda}$ by NEI results in

$$N = (t_I A_D \eta)\, NEI \qquad [e] \; , \tag{G-11}$$

where N = the total noise [e], and

NEI = the noise equivalent photon irradiance into the detector [$p/sec\text{-}cm^2$].

Taking the differential of Equation (G-5) gives

$$dE'_{\Delta\lambda} = \frac{\pi\tau_o}{4f^2_N}\, dL'_{\Delta\lambda} \qquad [p/sec\text{-}cm^2] \; . \tag{G-12}$$

Replacing $dE'_{\Delta\lambda}$ by NEI, and $dL'_{\Delta\lambda}$ by the noise equivalent photon radiance (NEPR) gives

$$NEI = \frac{\pi\tau_o}{4f^2_N}\, NEPR \qquad [p/sec\text{-}cm^2] \; . \tag{G-13}$$

Taking the differential of Equation (G-7) gives

$$dL'_{\Delta\lambda} = \tau_A\, dL'_{S\Delta\lambda} + \epsilon_A\, dL'_{A\Delta\lambda} \qquad [p/sec\text{-}cm^2\text{-}sr] \; . \tag{G-14}$$

However, since we are not interested in perturbations due to changes in the atmosphere, we assume $L'_{A\Delta\lambda}$ is to be constant. Equation (G-14) then becomes

$$dL'_{\Delta\lambda} = \tau_A\, dL'_{S\Delta\lambda} \qquad [p/sec\text{-}cm^2\text{-}sr] \; . \tag{G-15}$$

Replacing $dL'_{\Delta\lambda}$ with NEPR, and $dL'_{S\Delta\lambda}$ with the surface NEPR, $NEPR_S$ in Equation (G-15), gives

$$NEPR = \tau_A NEPR_S \qquad [p/sec\text{-}cm^2\text{-}sr] \; . \tag{G-16}$$

However, by definition,

$$dL'_{S\Delta\lambda} \equiv \frac{dL'_{S\Delta\lambda}}{dT_S} \, dT_S \qquad [p/sec\text{-}cm^2\text{-}sr] \tag{G-17}$$

or

$$dT_S = \frac{dL'_{S\Delta\lambda}}{\left(\dfrac{dL'_{S\Delta\lambda}}{dT_S}\right)} \qquad [K] \; . \tag{G-18}$$

Replacing dT_S with NEDT and $dL'_{S\Delta\lambda}$ with $NEPR_S$ in Equation (G-18) yields

$$NE\Delta T = \frac{NEPR_S}{\left(\dfrac{dL'_{S\Delta\lambda}}{dT_S}\right)} \qquad [K] \tag{G-19}$$

and

$$\frac{dL'_{S\Delta\lambda}}{dT_S} = \int_{\lambda_1}^{\lambda_2} \frac{dB(\lambda,T_S)\; d\lambda}{dT_S} \qquad [p/sec\text{-}cm^2\text{-}K] \; , \tag{G-20}$$

where the Planck function is given by

$$B'(\lambda,T_S) = \frac{C_1'}{\lambda^4} \, \frac{1}{\left[\exp\left(\dfrac{C_2}{\lambda T_S}\right) -1\right]} \qquad [p/sec\text{-}cm^2\text{-}sr\text{-}\mu m] \; . \tag{G-21}$$

Differentiating Equation (G-21) with respect to T_S yields

$$\frac{dB'(\lambda,T_S)}{dT_S} = \frac{C_2 \lambda^3 \left(B'(\lambda,T_S)\right)^2 \exp\left(\dfrac{C_2}{\lambda T_S}\right)}{C'_1 T_S^2} \qquad [p/sec\text{-}cm^2\text{-}sr\text{-}\mu m\text{-}K] \; . \tag{G-22}$$

Equation (G-19) may be written in terms of signal-to-noise ratio (S/N) as follows. Dividing Equation (G-1) by Equation (G-11) gives

$$\frac{S}{N} = \frac{E'_{\Delta\lambda}}{NEI} \quad [nd] \ . \tag{G-23}$$

Substituting Equations (G-5) and (G-13) into Equation (G-23) and replacing $dL'_{\Delta\lambda}$ with NEPR gives

$$\frac{S}{N} = \frac{L'_{\Delta\lambda}}{NEPR} \quad [nd] \ . \tag{G-24}$$

Substituting Equation (G-16) into Equation (G-24) gives

$$\frac{S}{N} = \frac{L'_{\Delta\lambda}}{\tau_A NEPR_S} \quad [nd] \tag{G-25}$$

or

$$NEPR_S = \frac{L'_{\Delta\lambda}}{\tau_A \left(\frac{S}{N}\right)} \quad [p/sec\text{-}cm^2\text{-}sr] \tag{G-26}$$

and, finally, by substituting Equation (G-26) into Equation (G-19), one obtains

$$NE\Delta T = \frac{L'_{\Delta\lambda}}{\tau_A \left(\frac{S}{N}\right)\left(\frac{dL'_S}{dT_S}\right)} \quad [K] \ . \tag{G-27}$$

NASA National Aeronautics and Space Administration

Report Documentation Page

1. Report No.
NASA RP-1241

2. Government Accession No.

3. Recipient's Catalog No.

4. Title and Subtitle
Sensor Performance Analysis

5. Report Date
July 1990

6. Performing Organization Code
625

7. Author(s)
H.E. Montgomery, H. Ostrow, and G.M. Ressler

8. Performing Organization Report No.
89B00057

10. Work Unit No.

9. Performing Organization Name and Address
Goddard Space Flight Center
Greenbelt, Maryland 20771

11. Contract or Grant No.

13. Type of Report and Period Covered
Reference Publication

12. Sponsoring Agency Name and Address
National Aeronautics and Space Administration
Washington, D.C. 20546-0001

14. Sponsoring Agency Code

15. Supplementary Notes
H.E. Montgomery and H. Ostrow: Sensor Concept and Development Branch, NASA-Goddard Space Flight Center, Greenbelt, Maryland, 20771.
G.M. Ressler: Ressler Associates, Inc., Laurel, Maryland 20724.

16. Abstract
This paper describes the theory and develops the equations required to design and analyze the performance of electro-optical sensor systems that operate from the visible through the thermal infrared spectral regions. Methods to compute essential optical and detector parameters, signal-to-noise ratio, MTF, and figures of merit such as NE$\Delta\rho$ and NEΔT are developed. A set of atmospheric tables are provided to determine scene radiance in the visible spectral region. The Planck function is used to determine radiance in the infrared. The equations developed in the paper have been incorporated in a spreadsheet so that a wide variety of sensor studies can be rapidly and efficiently conducted.

17. Key Words (Suggested by Author(s))
Spectral irradiance, detector responsivity, spectral radiance, dwell time, detector noise, noise equivalent delta reflectivity, noise equivalent delta temperature

18. Distribution Statement
Unclassified - Unlimited

Subject Category 43

19. Security Classif. (of this report)	20. Security Classif. (of this page)	21. No. of pages	22. Price
Unclassified	Unclassified	96	A05

NASA FORM 1626 OCT 86

NASA-Langley, 1990